Spring 2012

The use of electrical resistivity tomography (ERT) to delineate water-filled vugs near a bridge foundation

Jeremiah Chukwunonso Obi

Department:

THE USE OF ELECTRICAL RESISTIVITY TOMOGRAPHY (ERT) TO DELINEATE WATER-FILLED VUGS NEAR A BRIDGE FOUNDATION

by

JEREMIAH CHUKWUNONSO OBI

A THESIS

Presented to the Faculty of the Graduate School of the

MISSOURI UNIVERSITY OF SCIENCE AND TECHNOLOGY

In Partial Fulfillment of the Requirements for the Degree

MASTER OF SCIENCE IN GEOLOGICAL ENGINEERING

2012

Approved by

Neil Anderson, Advisor
David J. Rogers
Leslie Gertsch

ABSTRACT

A structural support was needed to strengthen the load-bearing capacity of an unnamed bridge foundation in Laclede County in South-Central Missouri due to increasing traffic volume and age of the bridge. This area is characterized by karstic features such as losing streams, underground caves and sinkholes. During the construction of a drilled shaft for the substructure, a few feet north of the north footing of the pier, voids were noted beneath a roughly 2 foot thick cap of dolomite rock. Because of this, there were concerns about the integrity of the rock beneath the existing bridge foundation.

Consequently, subsurface investigation was conducted at the site using borings. Results from the borings confirmed the presence of voids adjacent to or at the foundation bearing level of the northern and central pier footings. This information alone provides accurate data only at the sampling location, so control elsewhere has to be interpolated, which can result in erroneous interpretation. To map the lateral and vertical extent of the voids, electrical resistivity tomography (ERT) was employed using the SuperSting R8/IP Earth resistivity meter. The result obtained was used to complement the borehole information. Dipole-dipole electrode configuration was used. Based on the interpretation of the results of the ERT survey and borehole control, it was concluded that the bedrock in the area was mainly dolomite dipping from east to west, and appears to be competent bedrock. Voids encountered were not of room-sizes as to breach the integrity of the bridge foundation. Compaction grouting was the engineering solution employed to fill the voids and stabilize the ground around the structure.

ACKNOWLEDGEMENTS

My immense gratitude goes to Dr. Neil Anderson, my advisor for his invaluable contribution towards the success of this thesis. He directed and encouraged me to take up this topic. I also thank Dr. David J. Rogers and Dr. Leslie Gertsch for accepting to be on my committee. Their insightful comments and suggestions were great.

My special thanks go to my family and friends for their unflinching support and encouragement throughout my graduate studies.

TABLE OF CONTENTS

Page

ABSTRACT iii
ACKNOWLEDGMENTS iv
LIST OF ILLUSTRATIONS vii
LIST OF TABLES ix
SECTION
1. INTRODUCTION 1
1.1. OBJECTIVE 1
1.2. SITE DESCRIPTION 2
2. GEOLOGIC OVERVIEW OF STRATIGRAPHIC UNITS IN LACLEDE COUNTY, MISSOURI 5
2.1. BEDROCK DISTRIBUTION IN THE AREA 6
2.1.1. Ordovician System 6
2.1.2. Canadian Series 7
2.1.2.1. Gasconade formation 7
2.1.2.2. Roubidoux formation 8
2.1.2.3. Jefferson City formation … 8
2.1.2.4. Cotter formation 9
2.2. SURFICIAL MATERIALS IN LACLEDE COUNTY, MISSOURI 9
2.3. FAULTING 10
3. THEORY OF KARST FORMATION 11
4. GEOPHYSICAL APPLICATION 16
4.1. GEOPHYSICAL TOOLS USED TO MAP VOIDS AND CAVES 17
4.1.1. Ground Penetrating Radar (GPR) Method 17
4.1.2. Gravity Method 17
4.1.3. Electromagnetic Method (EM) 18
4.1.4. Seismic Reflection Method 18
4.1.5. Electrical Resistivity Tomography Method 19

5. LITERATURE REVIEW: ELECTRICAL RESISTIVITY TOMOGRAPHY (ERT) 20
5.1. CURRENT FLOW IN THE SUBSURFACE 21
5.2. RELATIONSHIP BETWEEN GEOLOGY AND RESISTIVITY 22
5.3. OHM'S LAW AND RESISTIVITY 23
5.4. THEORETICAL DETERMINATION OF RESISTIVITY 24
5.5. APPARENT RESISTIVITY 28
5.6. ELECTRICAL RESISTIVITY ARRAY CONFIGURATION 30
5.7. 2-D RESISTIVITY ARRAYS 30
6. DATA ACQUISITION 34
6.1. EQUIPMENT USED FOR ERT 38
6.2. ELECTRICAL RESISTIVITY TOMOGRAPHY DATA PROCESSING 40
6.3. RESOLUTION LIMITATION OF ERT METHOD 47
7. DATA INTERPRETATION 49
7.1. GENERAL GUIDE TO ERT DATA INTERPRETATION 50
7.2. ENGINEERING SOLUTION APPLIED 58
8. CONCLUSION 61
BIBLIOGRAPHY 63
VITA 65

LIST OF ILLUSTRATIONS

Figure Page

1.1. Location of the project site in Laclede County, Missouri. 3

1.2. Data acquisition of ERT at the site and the nature of the site 4

2.1. Fault pattern in southwestern Missouri (geosphere.gsapubs.org) 10

3.1. Karst map of the US published by AGI (Veni et al., 2001) 11

3.2. Stages of sinkhole formation 14

3.3. Nature of a fully developed sinkhole (http://news.nationalgeographic.com) 15

3.4. Karst feature near bridge pier at the project site. 15

5.1. Electric circuit for illustration of Ohm's Law. 24

5.2. Current lines radiating from the source and converging on the sink electrodes. 25

5.3.Current lines and equipotential surfaces in a medium of uniform resistivity 27

5.4. Current electrodes A and B and potential electrodes M and N 28

5.5. The most common electrode array configurations 31

6.1. Data acquisition of profile 1 34

6.2. Data acquisition of profile 2 35

6.3. Data acquisition of profile 5. 35

6.4. Sketch of electrical resistivity traverses at project site. 36

6.5. General site plan 37

6.6. Earth resistivity meter-SuperSting R8/IP, product of Advanced Geosciences Inc.. ..39

6.7. Electrical resistivity dipole-dipole array configuration used in the field 39

6.8. Example of a data set with a few bad data points (Loke, 2004). 41

6.9. Arrangement of the blocks used in a model together with the data points. 42

6.10. Unedited/raw profile 1 43

6.11. Unedited/raw profile 2 44

6.12. Unedited/raw profile 3 45

6.13. Unedited/raw profile 4 46

6.14. Unedited/raw profile 5 47

7.1. Interpreted profile 1 52

7.2. Interpreted profile 2 53

7.3. Interpreted profile 3 54

7.4. Interpreted profile 4 55

7.5. Interpreted profile 5 56

7.6. Lineament showing horizontal bedding plane.....60

LIST OF TABLES

Table Page

2.1. Geologic and stratigraphic units in Laclede County (Vandike, 1993).....5

5.1. Resistivity of common Earth's materials (Robinson, 1988) 22

7.1. Summary of results of boring logs at the project site 50

7.2. Summary of sizes of voids and volume of grout used to seal the voids 58

1. INTRODUCTION

1.1. OBJECTIVE

A structural support was needed to support an unnamed bridge foundation located in Laclede County in South-Central Missouri. The purpose for the construction of this structural support for the existing bridge was to strengthen the load bearing capacity of the bridge due to increasing volume of traffic and age of the bridge.

During the construction of a drilled shaft for the substructure, a few feet north of the footing of the pier 6, voids were noted beneath a roughly 2-foot-thick cap of dolomite rock. Because of this, there were concerns about the integrity of the rock beneath the existing bridge foundation. Background information obtained from borings confirmed the presence of voids adjacent to or at the foundation bearing level of the northern and central pier footings.

The geophysical laboratory at the Missouri University of Science and Technology (MS&T) was contracted to carry out a geophysical investigation of the project site to map the lateral and vertical extent of the voids detected near the pier. The result of the investigation had to be compared with the existing boring results for ground truth. This would ensure that subsurface conditions that would affect the integrity of the bridge foundation were detected and proper engineering solution such as compaction grouting employed.

With this task in mind, electrical resistivity tomography (ERT) method was deemed the appropriate geophysical tool to be employed for this project because it has proven to be an effective tool in mapping hidden karst features especially in areas with

highly variable elevation of bedrock. Data acquisition using electrical resistivity tomography is automated. The interpretations are normally highly reliable if constrained with borehole data. Also, proper use of this technique for karstic voids can often help geotechnical engineers develop an effective program of test borings and grouting, since if the bore spacing is greater than the cavity dimensions, it is possible to miss the cavity completely. Bedrock voids, whether filled with air, water, or sediment, constitute "missing mass" in comparison to solid rocks.

1.2. SITE DESCRIPTION

The project site is located in Laclede County, South-Central Missouri. It is part of the Ozark Highland Area. The area is known for the development of karstic feautures such as caves, springs, and sinkholes. The sinkholes that frequently develop on the broad, prairie-like uplands vary from broad bowl-shaped depressions encompassing several acres to steep-walled pits over 50 feet (15.2m) deep and 400 feet (121.9m) wide .

The area is underlain by sedimentary rocks of Ordovician age, namely the Gasconade Formation, the Roubidoux Formation, Jefferson City Formation and Cotter Formation. The Gasconade Formation is overlain by the Roubidoux Formation which is overlain by the Jefferson City Formation that caps the upland in the project site. These sedimentary strata are generally flat-lying. There is an area where the sloping valley floor intercepts the Gasconade Formation directly upstream of the project site. The Gasconade Formation is predominantly light brownish cherty dolomite, and consists of upper Gasconade dolomite and lower Gasconade dolomite.

The Roubidoux Formation consists of dolomite, cherty dolomite, sandy dolomite and dolomitic sandstone.

The Jefferson City Formation consists primarily of medium to finely-crystalline dolomite. The location of the project site is shown in Figure 1.1.

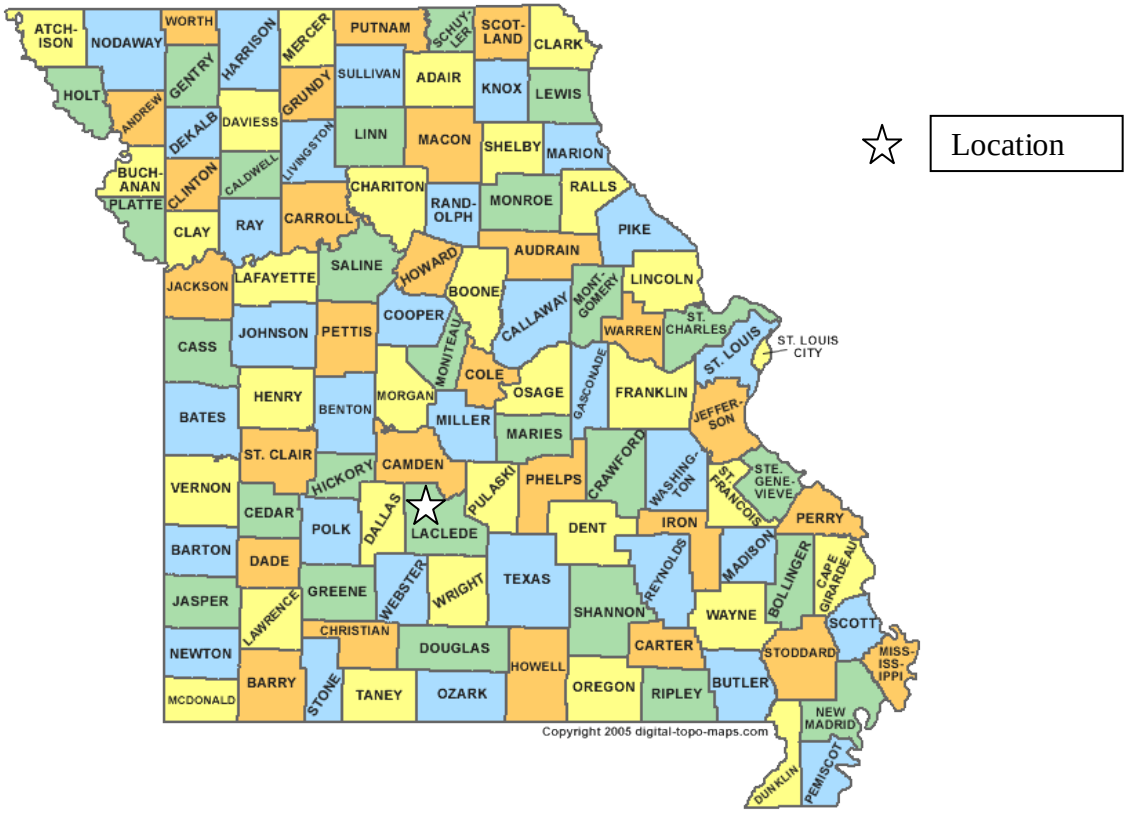

Figure 1.1. Location of the project site in Laclede County, Missouri

The project site is underlain mainly by the Gasconade Formation (Lower Gasconade Dolomite and Upper Gasconade Dolomite) and Roubidoux Formation, according to information from literature and types of rocks and rock samples collected from the site. The project site has an undulating topography with majority of the sloped

areas covered with grasses, shrubs and trees. The area is covered mostly by alluvium; weathered or eroded particles of minerals which are transported by a river and deposited usually temporarily at points along the flood plain of a river. The alluvium consists of chert gravels and cobbles interbeded with clay, silt, and sand. The cherty residuum is developed from weathering of dolomite, chert and sandstone. This type of geologic formation (Figure 1.2) is prone to sinkholes, losing streams, caves, and springs.

Figure 1.2. Data acquisition of ERT at the site and the nature of the site

2. GEOLOGIC OVERVIEW OF STRATIGRAPHIC UNITS IN LACLEDE COUNTY, MISSOURI

The geologic overview of the stratigraphic units in Laclede County, Missouri presented here is based on work of Martin, et al. (1961). The geologic and stratigraphic units of the study area belong to the Ordovician System and specifically the Canadian series as presented in Table 2.1.

Table 2.1. Geologic and stratigraphic units in Laclede County (Vandike, 1993)

System	Series	Group	Formation		Regional Thickness (ft.)
Mississippian	Osagean		Burlington-Keokuk Formation		150-270
			Elsey Formation		25-75
			Reeds-Spring Formation		125
			Pierson Formation		90
	Kinderhookian	Chouteau	Northview Formation		5-80
			Compton Formation		30
Ordovician	Canadian		Cotter Formation		
			Jefferson-City Formation		600
			Rubidoux Formation		150
			Gasconade Formation	Upper Gasconade Dolomite	350
				Lower Gasconade Dolomite	
				Gunter Sandstone Member	25

Table 2.1. Cont'd. Geologic and stratigraphic units in Laclede County (Vandike, 1993)

System	Series	Group	Formation	Thickness (ft.)
Cambrian	Upper		Eminence Formation	500
			Potosi Formation	
		Elvis	Derby-Doerun Formation	
			Davis Formation	150
System	Series	Group	Formation	Thickness (ft.)
			Bonneterre Formation	200
			Lamotte Formation	150
Precambrian	Crystalline rock			

2.1. BEDROCK DISTRIBUTION IN THE AREA

The geologic and stratigraphic succession in Missouri presented here is based on the work of James A. Martin, Robert D. Knight, and William C. Hayes, "The Stratigraphic succession in Missouri", 1961. The project site belongs to Ordovician System and Canadian Series and is described as follows:

2.1.1. Ordovician System. Rocks of Ordovician age are exposed over approximately one-third of the state of Missouri and attain aggregate thickness of approximately 3,800 feet (1158.2m). They crop out chiefly in the southern, eastern, and central parts of the state where they lie around the flanks of the Ozark Dome, sloping downward from the center in all directions. There are unconformities at both the base and the top of the system, with many significant unconformities being recognized as series and stage boundaries within the system. There are Canadian Series, the Champlainian Series, and Cincinnatian Series in the state that make up the Ordovician System. The

Canadian Series is one of the most extensive series represented in the state. The project site belongs mainly to the Canadian Series.

2.1.2. Canadian Series. The rocks of the Canadian Series in Missouri are principally arenaceous and consist of cherty dolomite and sandstone. They immediately underlie the surface in a large part of the state south of the Missouri River. They are bounded at the base and top by regional unconformities. Four bedrock Formations are present in this series; all of them represent the Canadian Series of the Ordovician System of Paleozoic Era. The bedrock formations, from oldest (lowest) to youngest, are described as follows, based on reconnaissance mapping by Middendorf and Thompson (1987) and Duley et al.1992).

2.1.2.1. Gasconade formation. The Gasconade is predominantly a light brownish-gray, cherty dolomite. There is also a persistent sandstone unit in its lowest part that is called the Gunter Member. The Gasconade Dolomite is typically light gray in color, medium to coarsely - crystalline, thin to thick - bedded, cherty dolomite, and is divisible into two units. The upper unit is a massively-bedded and relatively chert-free dolomite that forms bluffs and pinnacle glades. It is medium to coarsely crystalline, and weathers to a coarsely-pitted surface. It contains brown chert nodules or stringers with some druses. Thickness of the upper unit ranges from 40 to 70 feet (12.2 to 21.3m). The lower unit contains 30 to 50 percent chert and is light gray, medium-to coarsely crystalline dolomite with thin beds or nodules of white to gray porcelaneous chert and thin beds of silicified oolites. Cryptozoan reef structures are common and the top of the lower part is marked by a persistent, locally silicified cryptozoan reef 2 to 8 feet (0.6 to 2.4m) thick. The formation is about 300 to 350 feet (91.4 to 106.7m) thick, but in the

project area, only the upper 50 to 100 feet (15.2 to 30.4 m) are exposed in valleys bordering major rivers.

2.1.2.2. Roubidoux formation. The Roubidoux formation consists of sandstone, dolomitic sandstone, and cherty dolomite. The sandstone is composed of fine-to medium-grained quartz sand which characteristically is sub rounded and frosted. Gray and brown colors are predominant on weathered surfaces, but the color of the fresh sandstone is commonly light yellow, tan, or red at the surface and white in the subsurface. The dolomite in the Roubidoux Formation is finely crystalline, light gray to brown in color, and thinly to thickly bedded. Individual beds contain brown to gray, banded, oolitic, sandy chert. White to dark-gray or brown chert is present as irregular layers, nodules, and lenses in the dolomite. Cryptozoan reef structures are present locally as concentrically banded chert masses up to 2 feet (0.6m) in diameter. Near the basal contact, brecciated chert masses weather to boulders and blocks. The unit is about 120 to 150 feet (36.6 to 45.7m) thick.

2.1.2.3. Jefferson City formation. The Jefferson City formation is composed principally of light brown to brown, medium to finely crystalline dolomite and argillaceous dolomite. It typically contains banded chert nodules or thin seams of white to light-gray chert with some generally discontinuous lenses of shale and fine-to medium grained, poorly sorted white to light-gray sandstones up to 6 inches (0.15m) thick. A persistent marker bed, 15 to 20 feet (4.6 to 6m) thick, of brown and gray-mottled, medium-crystalline, thick-bedded dolomite weathers to a distinctive coarsely-pitted ledge. This occurs about 30 feet (9.1m) above the base. The thickness of the Jefferson

City Formation ranges from 125 to 350 feet (38.1 to 106.7m); its average thickness is about 200 feet (61m).

2.1.2.4. Cotter formation. The Cotter formation is composed mainly of light gray to light brown, medium to finely crystalline, cherty dolomite. It contains thin intercalated beds of green shale and sandstone. It is normally medium to thinly bedded.

2.2. SURFICIAL MATERIALS IN LACLEDE COUNTY, MISSOURI

Surficial materials are defined as all solid earth materials (clay, silt, sand, gravel and boulders) between the land surface and the top of bedrock (Vandike et al. 1992). In the project area, the dominant surficial material is residuum, a product formed from the disintegration and decomposition of Ordovician-age cherty dolomite and sandstone from Gasconade Formation. Other surficial materials in this area are

- loess; wind-deposited, clayey silt.
- colluvium; sediment eroded and transported down slope by gravitational forces,
- lag gravel; an accumulation of stones on an old surface from which the clay matrix has been eroded.
- alluvium; waterborne sediments of clay, silt, sand and gravel deposited in stream channels and flood plains.

On the uplands, a composite surficial material profile consists of a thin layer of loess on the surface, underlain by colluvium, lag gravel, residuum, and bedrock. The distribution and thickness of surficial materials are controlled by topography, weathering, erosion, and bedrock.

2.3. FAULTING

A distinctive pattern of faults crosses the area in a northwesterly trend; a less well-defined series of faults crosses in a northeasterly trend (Vandike et al. 1992). The faults have been inactive for millions of years, but weathering of bedrock along them has produced a pattern of northwest-trending, solution-enlarged joints and fractures that may control groundwater movement. Many of the river and creek channels have also developed a northwesterly trend that reflects the primary fault direction. The Reelfoot fault is the fault that trends northwest across the area as shown by black lines in Figure 2.1.

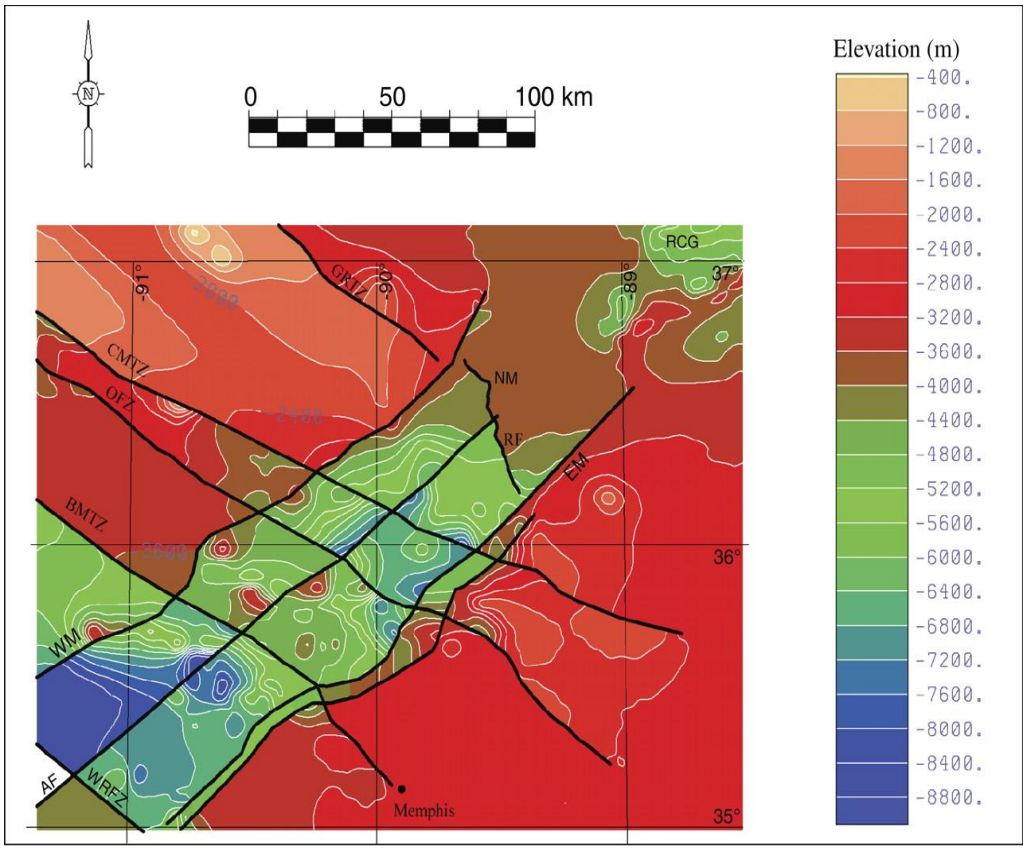

Figure 2.1. Fault pattern in southwestern Missouri (geosphere.gsapubs.org)

3.THEORY OF KARST FORMATION

The general representation of U.S. Karst areas published by American geological institute (AGI) (Veni et. al., 2001) indicates that almost all southern Missouri is underlain by carbonate rocks and recognized as a Karst terrain (shown in green color with star symbol on the map, Figure 3.1).

Figure 3.1. Karst map of the US published by AGI (Veni et al., 2001)

Karst is a term used to describe areas where the dissolving of soluble bedrock by groundwater and surface water has played a dominant role in developing topographic and drainage features. Karst features include sinkholes, losing streams, caves and springs. Sinkholes are bowl-shaped depressions in the landscape resulting from solutional activity underground.

Carbonate rocks (limestone and dolostone) are predominantly composed of calcite mineral ($CaCO_3$) and dolomite mineral ($CaMg\ (CO_3)_2$), and both, especially calcite, dissolve in slightly acidic waters; the dissolved materials, along with the remaining insoluble parts of the rock, are transported from the site through solution enlarged openings in the bedrock. Over time, a void or opening develops in the shallow subsurface that enlarges to the point where its roof can no longer sustain its own weight, and a collapse occurs. If the void develops mostly in surficial materials and not bedrock, the resulting sinkhole will initially have nearly vertical or overhung sides with little or no bedrock exposed in the walls.

These materials are eroded by run-off from rainfall, eroding materials from the rim of the sinkhole to form typical bowl-shaped depressions. In some cases the collapse occurs within a cave passage or void developed in bedrock. In this case the shape of the resulting sinkhole is more dependent on the configuration of the bedrock void. The sinkhole may contain vertical bedrock walls along parts or all of its perimeter, and may contain an enterable cave passage. The vast majority of sinkholes in the study area and its environs are developed in surficial materials, and few have bedrock walls. Sinkholes can be found in any of the four geologic formations exposed in this area, but are most

commonly developed in deeply-weathered Roubidoux Formation and Jefferson City Dolomite.

Stages of sinkhole formation are illustrated in Figure 3.2. The illustration is conceptual, meaning that actual conditions in nature may vary. For instance, the rock and soil layers may be thicker or thinner, the fractures and cave passages may be larger or smaller, and surfaces are likely to be much more irregular in shape. The stages are described as follows (www.dnr.mo.gov/.../geores/sinkholeformation.htm):

- Stage 1 –The opening in the bedrock surface allows overlying soil to move downwards into a cave passage. In this case the solution-widened fracture in the bedrock is choked with soil.
- Stage 2 – The collected soil from stage one is carried away by flowing water.
- Stage 3 – Soil in the fracture or bedrock opening collapses into the cave or is washed into the cave by water movement from the soil into the cave.
- Stage 4 – Voids form at the bedrock due to additional soil movement or collapse.
- Stage 5 – There is upward movement in the soil profile as a result of enlargement of the void. This process is known as stopping.
- Stage 6 – The void enlarges eventually until only a thin layer of soil remains at the surface.
- Stage 7 – The thinned soil roof can no longer support itself, thereby creating a surface collapse that may or may not choke the hole in the bedrock.
- Stage 8 – If the bedrock throat of the sinkhole remains plugged with the collapsed soil, the surface hole may fill with other eroded soil. If the steep surface is unstable, the hole may widen into a conical depression. If the throat is plugged

with soil, water may pond in the depression, forming a sinkhole lake. A fully developed sinkhole is typically funnel-shaped (Figure 3.3) and forms one of the signs of karst features observed at the project site (Figure 3.4).

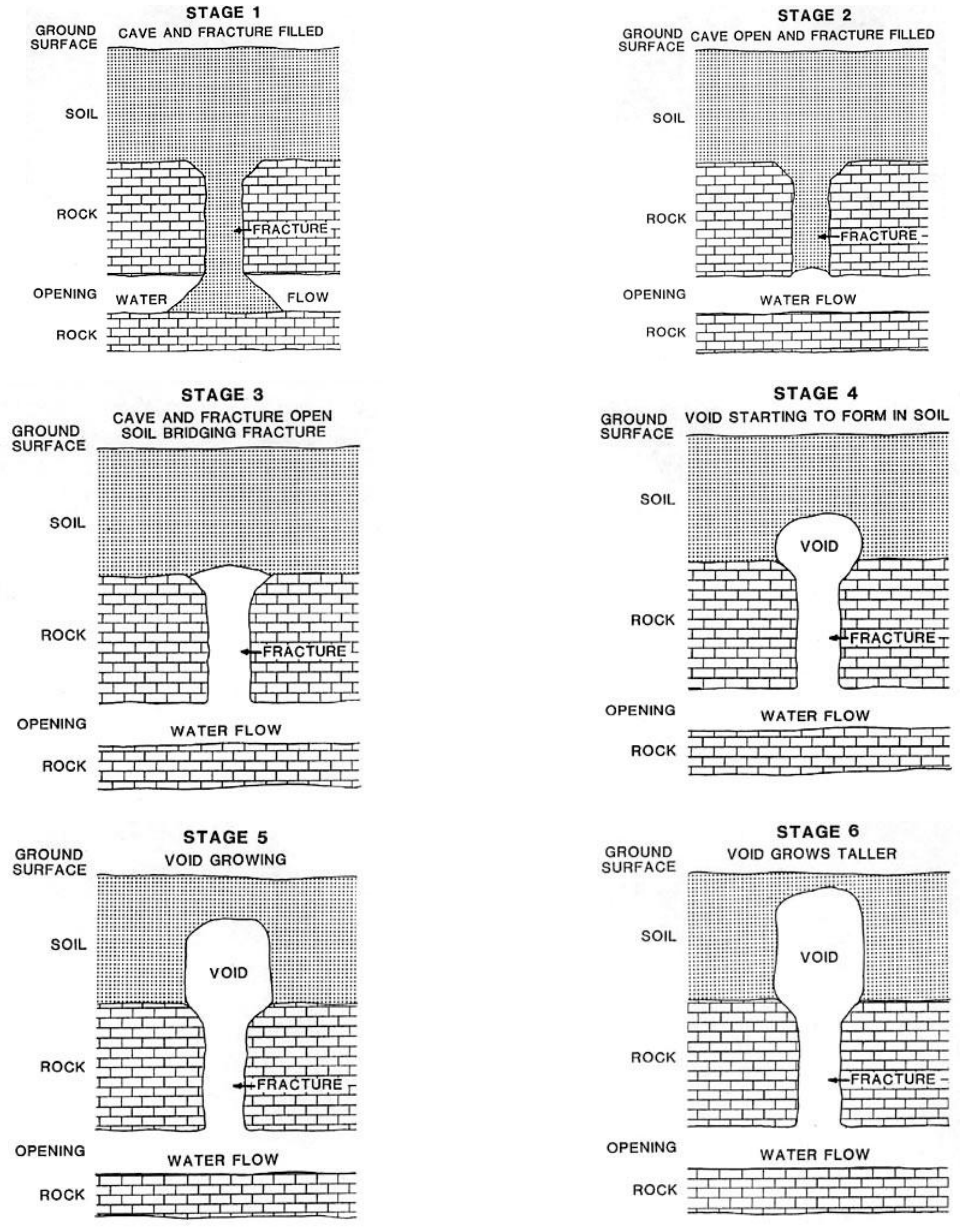

Figure 3.2. Stages of sinkhole formation
(www.dnr.mo.gov/.../geores/sinkholeformation.htm)

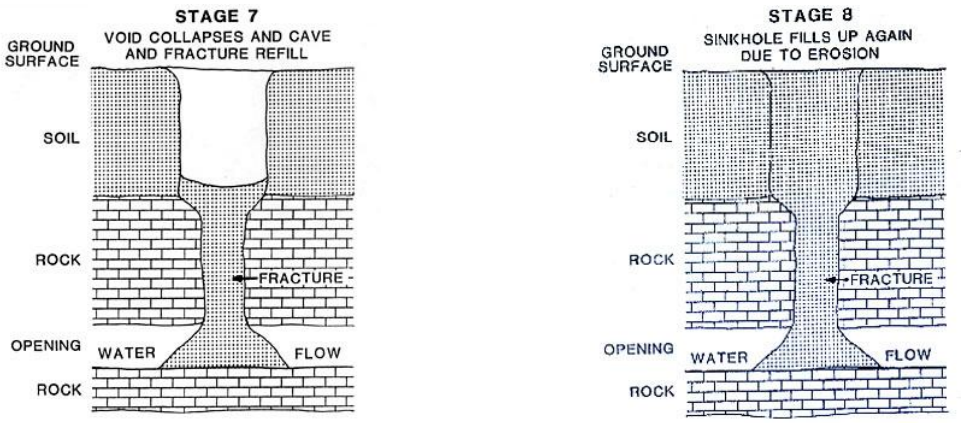

Figure 3.2 Cont'd. Stages of sinkhole formation

Figure 3.3. Nature of a fully developed sinkhole (http://news.nationalgeographic.com)

Figure 3.4. Karst feature near bridge pier at the project site

4. GEOPHYSICAL APPLICATION

Geophysical methods employ indirect, non-intrusive observations to characterize and map variations in the physical properties of what lies concealed beneath the ground surface. According to the Encycoledia of Caves and Karstic Science, 2004, "All geophysical techniques require contrasts of some physical properties (density, electrical resistivity, magnetic susceptibility and seismic velocity) between subsurface structures. Although void space in rock may represent an enormous contrast in physical properties that can be advantageous to an investigator seeking concealed caves, underground karst openings are frequently small, irregular targets whose effects are easily masked by those of surface irreglarities. In deep exploration, techniques that are useful usually are at the expense of resolution and accuracy; conversely, techniques capable of generating high-resolution images of shallow features are often based on high-frequency signals that are rapidly attenuated as they propagate through deeper soil and rock".

It is conventional in geotechnical engineering practice to obtain subsurface information before embarking on any project. Mapping hidden karst is necessary when engineering projects are planned in rock formations known to contain caves, because karstic voids and collapses can compromise the integrity of building foundations, dams, and bridges. Drilling of boreholes is one of the methods of obtaining subsurface information. But if detailed subsurface information is needed, boreholes have to be closely spaced in order to produce a reliable image of the subsurface. Unfortunately, such drilling of multiple boreholes is time-consuming and uneconomical. More so, even though the subsurface information obtained at boring location is very accurate, the

interpolation between boreholes can sometimes be erroneous due to significant variations in karst terrain. Use of geophysical tools as a control reduces the number of required boreholes and significantly decreases the ambiguity of the subsurface conditions.

4.1. GEOPHYSICAL TOOLS USED TO MAP VOIDS AND CAVES

Some of the common geophysical techniques that can be used to detect caves and karstic voids are electrical resistivity, ground penetrating radar (GPR), gravity, electromagnetic (EM), and seismic reflection. All these methods have their strengths and weaknesses, so the choice of method to use depends on a number of factors such as the size and depth of anticipated voids, reason for delineating voids, desired resolution of voids, nature of background materials or bedrock surrounding the voids, type of materials that may fill the voids (such as clay or water), depth to groundwater, size of the investigation area and sources of cultural interference like power lines and fences in the investigation area.

4.1.1. Ground Penetrating Radar (GPR) Method. In ground penetrating radar (GPR) method, pulses of electromagnetic energy penetrate the ground and are partially or totally reflected from rock or soil boundaries with contrasting electrical properties (notably their dielectric constants, or permittivity). Air-filled voids and layers of water-saturated sediment are strong radar reflectors. The reflected signals are detected on the ground surface and are collated by computer to produce the ground profiles. But clay-rich soils attenuate GPR signals and can restrict depth investigation to just 1foot (0.30m).

4.1.2. Gravity Method. In gravity method, the negative density contrast between the target and the surrounding earth materials is identifiable as a local reduction in the

Earth's gravitational acceleration (g) measured at the surface. Gravity surveys can distinguish heavily karstified zones from nearby areas with a lower overall void space, but gravity tells us little about the size and shape of individual voids. Also, interpretation of gravity anomaly is limited by ambiguities; voids may still be present where no anomaly is detected due to coincidental combination of additive and negative anomalies. Another drawback is that gravity data needs a lot of corrections such as topography, elevation, latitude and tidal corrections. All these have to be applied to the data before they can be modeled.

4.1.3. Electromagnetic Method (EM). Electromagnetic method (EM) also uses electromagnetic waves that are transmitted into the ground. Where the waves encounter electrical conductors in the ground, they induce electrical currents in these conductors, which in turn generate electromagnetic waves that can be collected at the surface by an antenna. It can be useful in clay and water-filled voids. Its limitations are that air-filled voids or fractures are transparent to electromagnetic signal and are difficult to detect. Another major limitation of EM is ambiguity, because it may be difficult to isolate changes in depth to bedrock from lateral changes in electrical conductivity.

4.1.4. Seismic Reflection Method. Seismic reflection surveys can detect voids because the large negative reflection coefficient that exists between air and rock, or water and rock, generates an echo that is strong and reverses the phase of the signal. Single sets of ground-based seismic data have often failed to produce interpretable results, but tomographic sections (imaging by sections or layers) have proved more useful. The major limitation is that it demands expensive exploration infrastructure such as computer analysis of large banks of data and incorporation of boreholes.

4.1.5. Electrical Resistivity Tomography Method. Electrical resistivity method utilizes contrasting electrical properties to characterize and map buried rock. Electrical current is transmitted directly into the ground through a pair of electrodes, which results in a voltage change measured between a second pair of electrodes. The apparent resistivity (ρ_a) of the ground can be calculated, and since low porosity bedrock usually exhibits an electrical resistivity higher than overlying sediment, the buried topography can be interpreted. Electrical resistivity can map lateral and vertical variations in apparent resistivity of geologic material. It can approximate the size, shape and depth of air-filled caves.

5. LITERATURE REVIEW: ELECTRICAL RESISTIVITY TOMOGRAPHY (ERT)

Tomography means using any kind of penetrating wave for sectional imaging of a structure or object, while the image produced is a tomogram. The method of using electrical resistivity to partition the earth based on varying resistive properties of the earth materials to produce a tomogram is called electrical resistivity tomography (ERT).

Electrical resistivity tomography (ERT) has proven to be an effective geotechnical and environmental engineering tool. It is widely applied in determining the depth to bedrock, locating of contaminated plumes, acquiring information on elevation of groundwater table, etc. This method is especially preferred for site characterization in karst terrains (Zhou, 1990). When electrical resistivity tomography is used in combination with exploratory boreholes, the cost and time required for project execution and completion can be significantly reduced. When the geophysical data are constrained by borehole control, they can provide accurate and high resolution interpretations. Also, the use of this geophysical method can be of immense help in terms of sitting additional borehole control.

Electrical resistivity tomography technique has been successfully used in different situations by numerous investigators (Anderson, et al., 2006; Hiltunen D. R. and Roth M. J. S., 2008; Garman, K. M. and Purcell, S. F., 2008; Loke, M. H., 2008; Zhou, et al., 2002; Zhou, et al., 2000; Hamzah, et al., 2006; Cardimona, S., 2008; Dong, et al., 2008) to assess karst terrains.

Electrical resistivity tomography when compared with other geotechnical investigation techniques such as trenching and borehole drilling proves to be rapid in

terms of data acquisition. It is also relatively inexpensive and less labor intensive. In karst terrains where lateral variations in the depth to bedrock vary greatly, interpolation of the subsurface conditions between two boreholes can often provide erroneous results. The use of electrical resistivity tomography (ERT) can provide more precise information on ground conditions between borehole locations. Also data can be obtained without interrupting investigated objects or area (Non-Destructive Test).

Like most engineering and geophysical techniques, electrical resistivity tomography (ERT) has its limitations and challenges. For example, if an area is covered by concrete or asphalt, it is difficult to plant the metal stakes used to connect electrodes to the ground for resistivity measurement to be taken. Also, vertical resolution of resistivity data tends to decrease with depth.

The basic concepts of electrical resistivity technique used for this project are described below.

5.1. CURRENT FLOW IN THE SUBSURFACE

Electrical current flow in the subsurface is primarily electrolytic. Electrolytic conduction involves passage of charged particles by means of groundwater. Charged particles move through liquids that infill the interconnected pores of permeable materials (Robinson, 1988). When an electrical resistivity tomography survey is conducted in karst terrain, current flow is generally assumed to be electrolytic rather than electronic.

5.2. RELATIONSHIP BETWEEN GEOLOGY AND RESISTIVITY

Variations in the resistivity of subsurface materials are mostly a function of lithology. Information about resistivity variations within the subsurface can be associated with different materials. Some resistivity values are given in Table 5.1.

Table 5.1.Resistivity of common Earth's materials (Robinson, 1988)

Earth Material	Resistivity, Average or Range (Ohm-m)	Earth Material	Resistivity, Average or Range (Ohm-m)
Granite	10^2-10^6	Sandstone	1-10^8
Diorite	10^4-10^5	Limestone	50-10^7
Gabbro	10^3-10^6	Dolomite	10^2-10^4
Andesite	$10^{2-}10^4$	Sand	1-10^3
Basalt	10-10^7	Clay	1-10^2
Peridotite	10^2-10^3	Brackish water	0.3-1
Air	~ ^{0}	Seawater	0.2

From Table 5.1, it can be noted that most materials are characterized by resistivity values that vary by several orders of magnitude. For example, limestone has resistivity values ranging from 50 ohm-m to 10^7 ohm-m. Most minerals are considered to be insulators or resistive conductors. So in the majority of rocks, electrical current flow is accomplished by passage of ions in pore fluids (electrolytic conduction). The conductivity, which is the inverse of resistivity, is mostly affected by porosity, saturation, salinity, lithology, clay content and to some degree by temperature. Accordingly, materials with constant mineralogical composition can possess different resistivity values, depending on all the above mentioned parameters.

5.3. OHM'S LAW AND RESISTIVITY

In 1872, George Simon Ohm derived empirical relationship between the resistance (R) of a resistor in a simple series circuit, the current passing through the resistor (I), and the corresponding change in potential (ΔV) :

$$\Delta V = I R \tag{5.1}$$

A simple series circuit that consists of a battery connected to a resistor by a wire demonstrates this relationship (Figure 5.1). By using Ohm's Law, the value of resistance (R) can easily be calculated by plugging values of voltage (ΔV) and current (I) in the equation (5.1). The last two values are given because they can be measured. The electrical resistivity tomography concept is based on this relationship (Equation 5.1), with the assumption that the resistor in the circuit (Figure 5.1) is the Earth.

There is another relationship that defines resistance (R) as a function of geometry of a resistor and the resistivity of the cylindrical-shaped body:

$$R = \rho L/A \tag{5.2}$$

This equation shows that the magnitude of resistance is affected by the length (L) and the cross-sectional area (A) (Figure 5.1) of the cylindrical-shaped body through which electrical current flows (resistor). A factor that defines the ease with which electrical current flows through the media is known as resistivity (ρ).

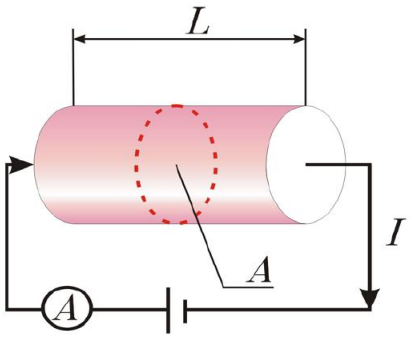

Figure 5.1.Electric circuit for illustration of Ohm's Law

By rearranging equation (5.2), the resistivity can be expressed as:

$$\rho = R\ A/L \qquad (5.3)$$

The electrical resistivity of any material is the resistance between the opposite faces of a unit cube of the material. Resistivity is an internal parameter of the material through which current is compelled to flow and describes how easily this material can transmit an electrical current. High values of resistivity imply that the material making up the wire is very resistant to the flow of electricity. Low values of resistivity show that the material making up the wire transmits electrical current very easily.

5.4. THEORETICAL DETERMINATION OF RESISTIVITY

The estimation of the apparent resistivity of the earth is relatively simple if several assumptions are made.

The first assumption is that a model-Earth is uniform and homogeneous, thus it possesses constant resistivity throughout the entire earth.

The second assumption is that the Earth is a hemispherical resistor in a simple circuit consisting of a battery and two electrodes (the source and the sink electrodes) pounded into the ground (Figure 5.2). The battery generates direct electrical current that enters the Earth at the source electrode connected to the positive portal of the battery. The current exists at the sink electrode coupled to the negative portal of the battery.

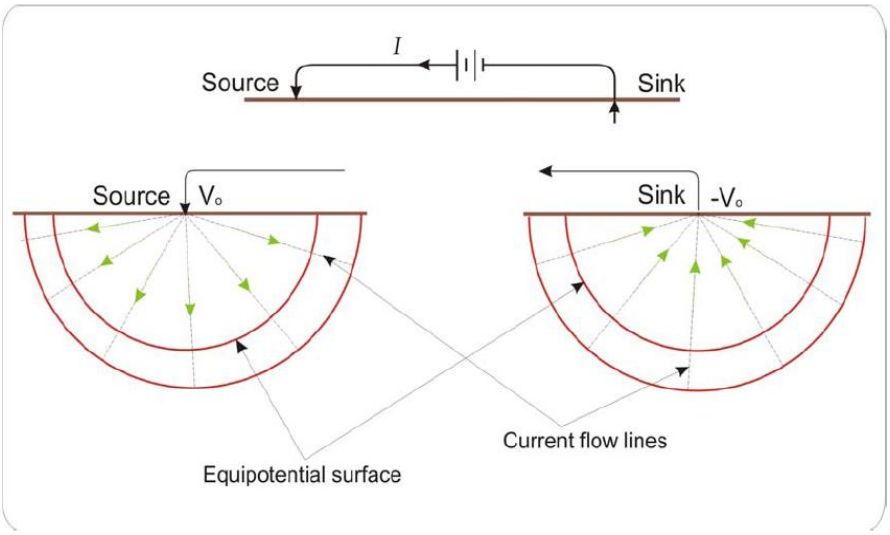

Figure 5.2.Current lines radiating from the source and converging on the sink electrodes (Edwin S. Robinson, 1989)

When the current is introduced to the ground, it is compelled to move outward from the source electrode. Due to the assumption that the earth is homogeneous, the current spreads outward in all directions from the electrode, and at each moment of time, the current front will move through a hemispherical zone. The area of such a hemispherical zone can be found from the relationship:

$$A = 2\pi d^2 \quad (5.4)$$

Where d is the distance from the source electrode to the point on the hemispherical surface defined by Equation (5.4), Figure 5.2.

By substituting equation (5.4) into equation (5.3), we can obtain an expression that defines the resistance of the media at a point separated from the source by distance d:

$$R = \rho / 2\pi d \quad (5.5)$$

The potential difference resulting from the flow of current through the hemispherical resistor can be found from combining Ohm's law expressed by Equation (5.1) and Equation (5.5):

$$V = I\rho/2\pi d = V_0 - V_d \quad (5.6)$$

Where V_0 is a potential at the source electrode and V_d is a potential at the surface of the hemisphere with radius d.

This equation demonstrates that for any point located at the hemispherical surface with radius d, the potential between this point and the source electrode is the same. Such a hemisphere is a surface of constant potential and is called an equipotential surface. In other words, the potential difference between a source and any point on the equipotential surface has the same numerical value.

When the two electrodes are at a finite distance from each other, the potential at any point M separated by distance d_1 from the source electrode, and distance d_2 from the sink electrode, can be found as the sum of the potential contributions from source and sink electrodes for point M (Figure 5.3).

$$I\rho/2\pi\,[1/d_1 - 1/d_2] \qquad (5.7)$$

This equation can be employed to calculate the potential point by point throughout the earth. By plotting these points and connecting those that are equal, the equipotential surfaces can be obtained (Figure 5.3).

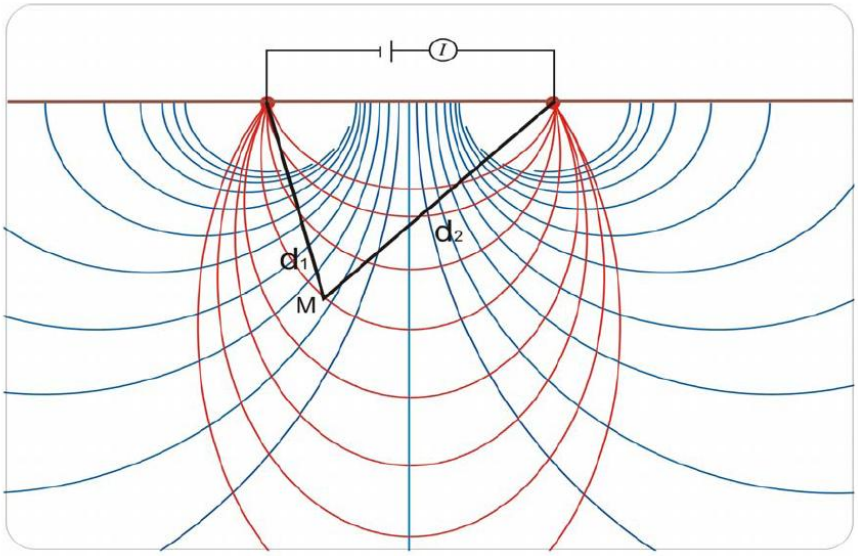

Figure 5.3.Current lines and equipotential surfaces in a medium of uniform resistivity (Edwin S. Robinson, 1989)

5.5. APPARENT RESISTIVITY

To acquire 2-D electrical resistivity tomography data in the field, a four- electrode array can be used. Two of these electrodes are used to inject electrical current into the ground and are referred to as current electrodes (Figure 5.4; indicated by letters A and B), and the other two electrodes are connected to a voltmeter and are used to measure the potential difference between electrodes (Figure 5.4; shown by letters N and M).

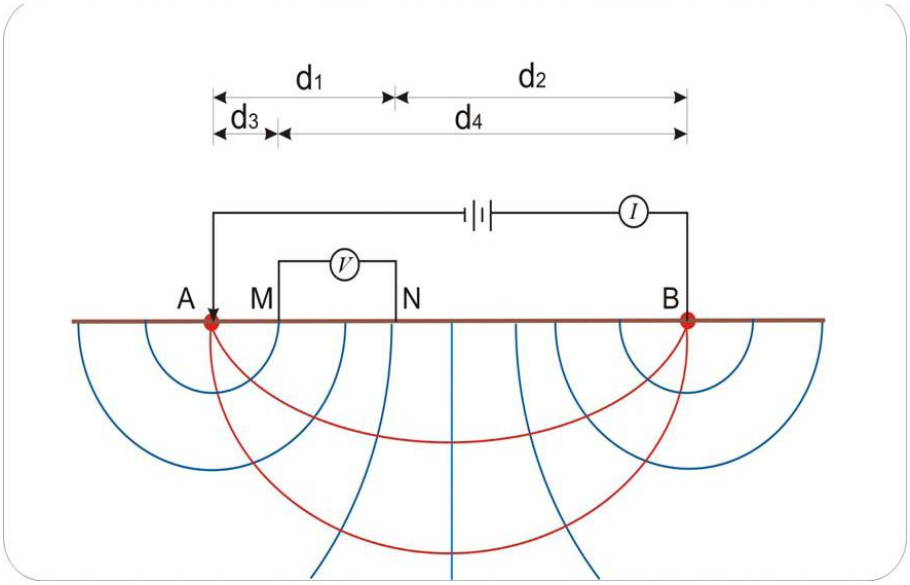

Figure 5.4. Current electrodes A and B and potential electrodes M and N

Current flow direction is shown by red lines and equipotential surfaces are indicated by blue lines. The assumption that the media through which the current is compelled to flow is homogeneous provides for a constant value of resistivity irrespective of where the voltmeter electrodes are placed.

Taking into account the geometry of the electrodes' configuration, as illustrated in Figure 5.4, the electric potential at point M can be deduced from the equation:

$$V_M = I\rho/2\pi\,[1/d_1 - 1/d_2] \quad (5.8)$$

$$V_N = I\rho/2\pi\,[1/d_3 - 1/d_4] \quad (5.9)$$

Therefore, the potential gradient between these two points, $V_{MN,}$ is

$$V_{MN} = V_M - V_N = I\rho/2\pi\,[1/d_1 - 1/d_2 - 1/d_3 + 1/d_4] \quad (5.10)$$

In practice, subsurface materials possess different physical characteristics, and the assumption that resistivity is the same everywhere is not true. Thus, resistivity values that are measured in the field are average resistivity values between two equipotential surfaces, and are known as apparent resistivity values ρ_a. It can be expressed as:

$$\rho_a = K * V_{MN}/ I \quad (5.11)$$

Where K is the geometric factor that depends on the electrode array configuration.

$$K = 2\pi/\,[1/d_1 - 1/d_2 - 1/d_3 + 1/d_4] \quad (5.12)$$

5.6. ELECTRICAL RESISTIVITY ARRAY CONFIGURATION

For modern electrical resistivity tomography surveys, multi-electrode systems are preferred. The greater the number of electrodes permanently attached to multi-core cable, the higher the investigation capabilities, and less time is spent in the field. Use of multi-electrode system allows combination of vertical sounding and horizontal profiling data to be collected simultaneously. Also it allows the generation of a two-dimensional model of resistivity distribution (Lateral and Vertical).

For 2-D imaging using a modern multi-electrode system, the spacing between electrodes stays fixed for the entire survey. Measurements are taken sequentially using different sets of four electrodes controlled by switching device. The depth of investigation is a function of the array type, the length of array and the physical parameters of material underlying the area of interest, and typically ranges from one-third to one- fifth of the length of the entire array (Robinson et al., 1988).

5.7. 2-D RESISTIVITY ARRAYS

Some of the more common electrode configurations such as Wenner array, Schlumberger array, and Dipole-dipole array are briefly discussed below. The geometry of an electrode array depends on the target depth, the time allowable for data acquisition, and the required spatial resolution.

When a multi-electrode system is used, the spacing between all electrodes remains the same, while the distance between current and potential electrodes depends on electrode configuration. This distance is controlled automatically by resistivity meter.

Most electrical resistivity tomography surveying is done with one of the electrode geometries illustrated in Figure 5.5.

For the 2-D Wenner Array (Figure 5.5), current and potential electrodes are separated by equal distance ‘a’ such that,

$$AM = MN = NB = a \tag{5.13}$$

All the electrodes are arranged along a continuous line, also known as survey line or traverse. The geometric factor for Wenner Array can be expressed as,

$$K_W = 2 * \pi * a \tag{5.14}$$

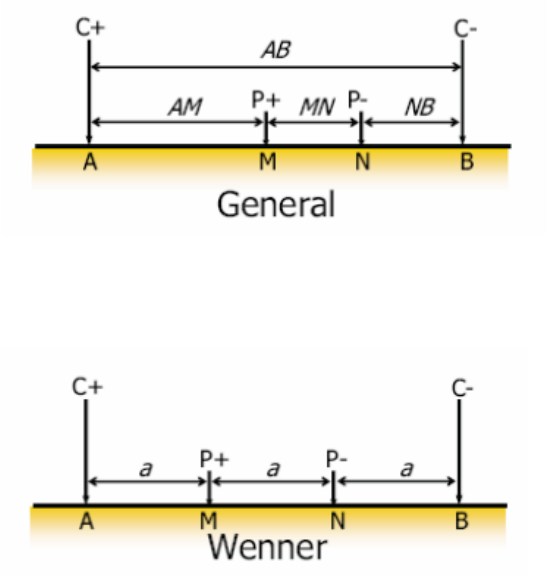

Figure 5.5. The most common electrode array configurations (http://pangea.stanford.edu/research/groups/sfmf/docs/DCResistivity.pdf).

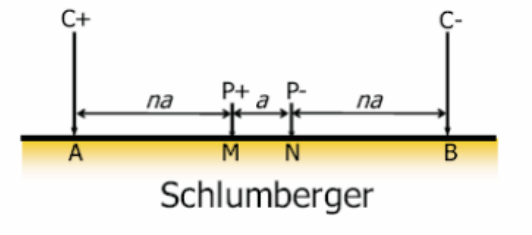

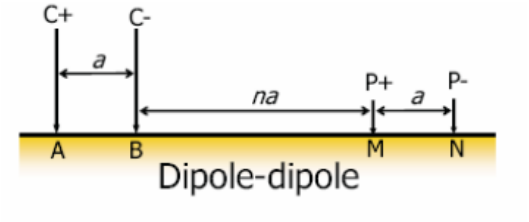

Figure 5.5. Cont'd. The most common electrode array configurations

For the 2-D Schlumberger array (Figure 5.5), the current electrodes A and B are located on the opposite sides from center point of the array .The passive electrodes N and M are placed between A and B electrodes.

Suppose the current electrodes A and B are separated by distance 'L ', and the passive electrodes N and M are separated from the center by distance 'b', the geometric factor for Schlumberger array can be given by the expression:

$$K_S = \pi (L^2 - b^2) /2b \qquad (5.15)$$

The third geometry is attributed to the Dipole - dipole configuration, where the potential electrodes M and N are not placed between the current electrodes A and B (Figure 5.5).

The Dipole - dipole array is logistically the most convenient array used in the field, especially for large scale projects. In this type of array, all four electrodes are placed along the same line, and the distance between the current electrodes A and B is equal to the distance between the potential electrodes M and N, represented by 'a', given by the following,

$$AB = MN = a \tag{5.16}$$

The distance between the middle points of current and the passive electrode sets is an integer multiple of a, and the factor itself is assigned to be equal to n (Figure 5.5).

The geometric factor K can be found from the following expression:

$$K_{DD} = \pi * n\,(n^2 - 1) * a \tag{5.17}$$

The dipole-dipole method was used in this project because this type of array has proven to be the most efficient in areas with great lateral variations in depth to bedrock (Zhou, 2000).

6. DATA ACQUISITION

The geophysical investigation was conducted towards the end of February 2011, when the average temperature was about 30 degrees F. The initial plan for the project was to run six electrical resistivity profiles; four would be parallel to the bridge pier in question and two traverses would be roughly perpendicular or at a skewed angle on either side of the bridge bent. The parallel profiles would be one on either side of the bridge pier. The first profile acquired was profile 1(Figure 6.1), and was close to profile 2 (Figure 6.2). Profile 5 (Figure 6.3) was roughly perpendicular to other profiles.

Figure 6.1. Data acquisition of profile 1

Figure 6.2. Data acquisition of profile 2

Figure 6.3. Data acquisition of profile 5

But after acquiring the fifth resistivity data set (profile 5), the equipment developed a fault, and the sixth data set (profile 6) could not be acquired. Profiles 5 and 6 were supposed to be the perpendicular profiles, so data interpretation was based on five profiles (profiles 1-5) as shown in Figure 6.4.

The site plan (Figure 6.5) shows the location of all the boreholes and resistivity profiles with respect to the bridge piers. Bridge pier 6 (C6) is the primary exploration target.

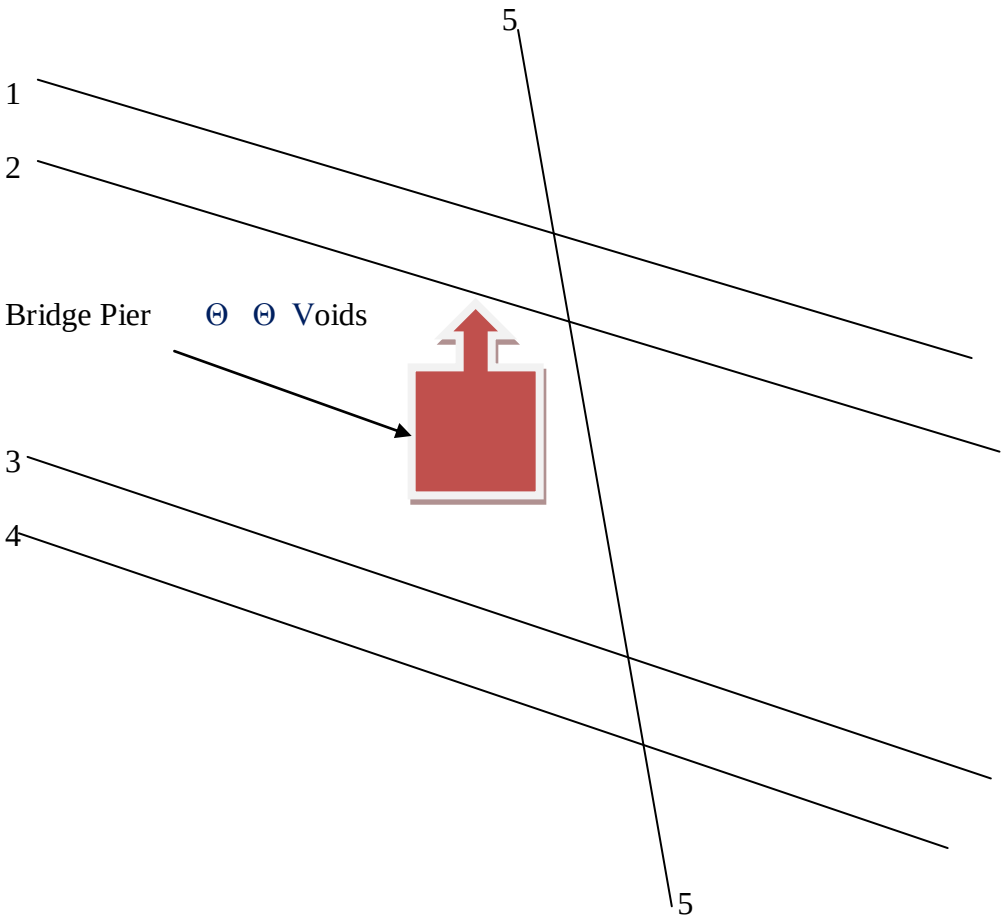

Figure 6.4. Sketch of electrical resistivity traverses at project site

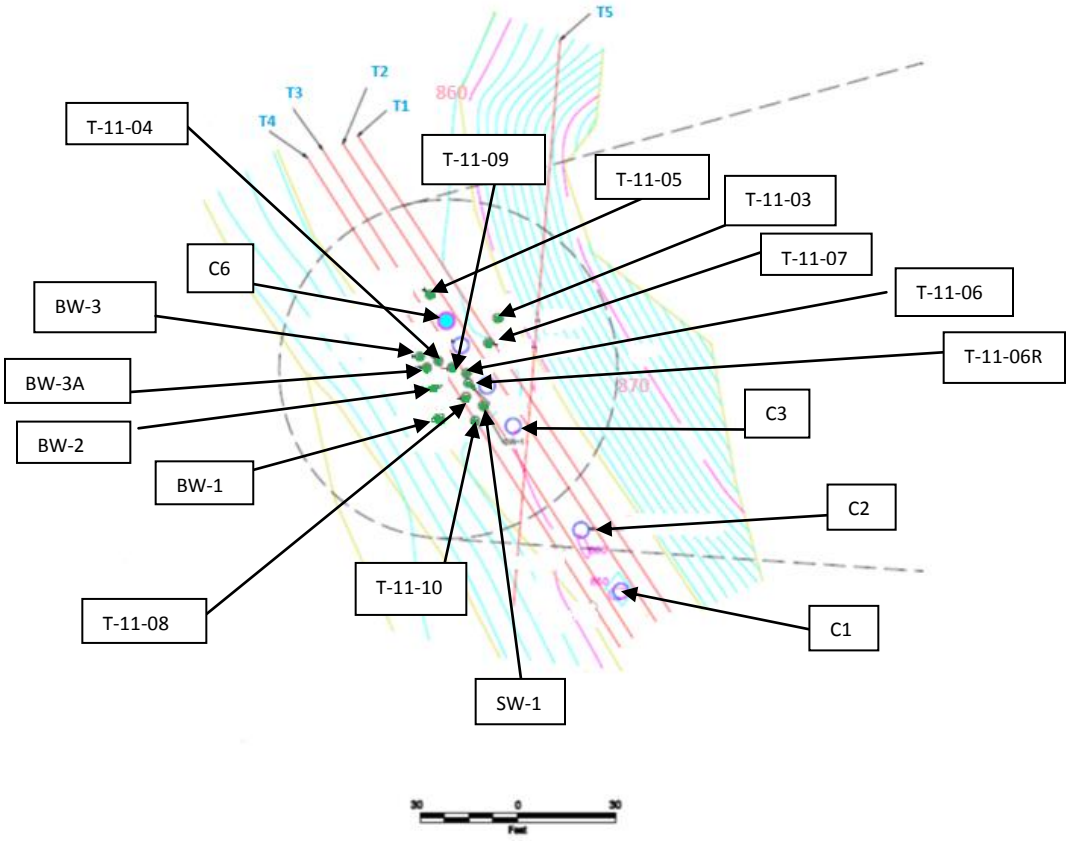

Figure 6.5. General site plan

Locations of fourteen boreholes drilled at the site are shown as green dots, C represents the bridge pier. Bridge pier C6 is the primary exploration target. Boreholes SW-1, BW-1, BW-2, BW-3 and BW- 3A are not logged. Boreholes T-11-03 to T-11-10 are logged boreholes. The five resistivity profiles are represented by T1, T2, T3, T4 and T5.

The electrical resistivity profiles were acquired using a SuperSting R8 resistivity unit with 72 electrodes spaced at 2.5 feet (0.76m) each for a total traverse length of about 177.5 feet (54.1m). The profiles were separated from one another by 4.5 feet (1.4m)

except profiles 2 and 3 which had a separation distance of about 7.5 feet (2.3m) due to presence of the bridge pier.

The SuperSting R8 resistivity unit makes use of dipole-dipole array configuration. This type of configuration is very sensitive to horizontal changes in resistivity (Zhou, 2007), which means that it performs well in mapping vertical structures such as vertically oriented solution-widened joints. A small electrode interval of 2.5 feet (0.76m) was chosen to ensure high resolution at the required depth of investigation. Each profile length was approximately 177.5 feet (54.1m) long and the profiles were separated from one another by 6 feet (1.82m) interval except profile 2 and 3 with separation distance of about 10.7 feet (3.26m) due to obstacle.

6.1. EQUIPMENT USED FOR ERT

Electrical resistivity tomography (ERT) involves introduction of electrical current into the subsurface by means of electrodes attached to the ground. All required measurements are by resistivity meter. For this project, a multi-channel portable memory Earth resistivity meter-SuperSting R8/IP, manufactured by Advanced Geosciences, Inc., (Figure 6.6) was used. The SuperSting was powered by a 12-volt battery. For larger scale projects, two batteries can be used.

Figure 6.6. Earth resistivity meter-SuperSting R8/IP, manufactured by Advanced Geosciences Inc.

For this project, seventy two (72) electrodes were connected to the insulated low resistance multi-core cable. Each electrode is tied to a metal stake pounded on the ground using a rubber - band, this allows electric current to flow from the electrode to the ground or subsurface. The electrodes are connected to the switching unit which also connects the SuperSting. Laptop computer is connected to the SuperSting, and the whole set up is powered by a 12- volt battery. Dipole - dipole array configuration was used.

In dipole - dipole array configuration, as shown in Figure 6.7, the electrodes are attached to a multi-core cable in a straight line.

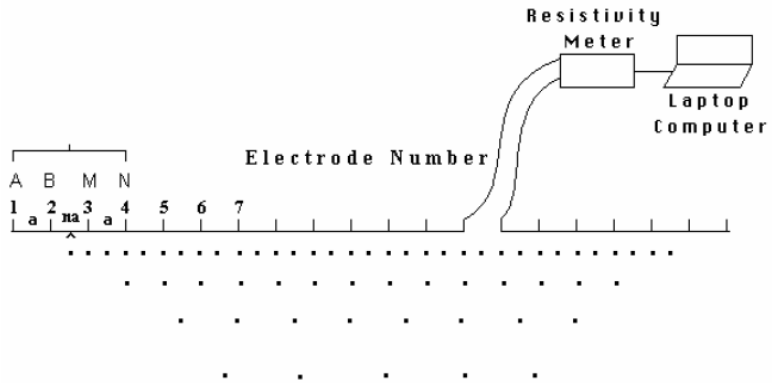

Figure 6.7. Electrical resistivity dipole-dipole array configuration used in the field

The cable is connected to the switching unit hardwired into the SuperSting resistivity meter. The unit controls the selection of the current (A&B) and potential (M&N) electrodes for each measurement. The SuperSting resistivity meter is connected to a laptop computer where the data is stored.

6.2. ELECTRICAL RESISTIVITY TOMOGRAPHY DATA PROCESSING

The resistivity data sets collected in the field were converted into resistivity models for interpretation of subsurface conditions using the RES2DINV software.

ERT data was processed using the following steps;

- Inspection of the resistivity data sets for presence of unreasonably high and low (negative) resistivity values called " bad data points" (Loke, 2004).
- Removal of "bad data points".
- Compilation of a resistivity model/ERT resistivity profile that displays horizontal and vertical resistivity distribution.

Before processing, the data acquired had to be inspected for presence of "bad data points" (Loke, 2004). "Bad data points" mean resistivities of unrealistically high or low (negative) values. "Bad data points" can be caused by several factors, such as failure during survey of equipment used, for example electrode malfunction. Also, very poor electrode - ground contact can result to "bad data points". In addition, when a metal stake attached to an electrode is driven into an ice lens, resistivity measurements are affected. Ice acts as an insulator, and affects resistivity measurements. This is a problem for surveys done in winter.

Inspection of “bad data points” is done by viewing a profile plot, illustrated in Figure 6.8. The “bad data points” appear as stand out points. All “bad data points” are marked as red plus signs. The RES2DINV software offers an option that allows for removal of such points manually by simply clicking on them. After the resistivity data sets acquired in the field were inspected and all unrealistic values removed, the RES2DINV software used an inversion algorithm to convert the measured resistivity model/ERT resistivity profiles to a geologic model which reflect lateral and vertical resistivity distribution.

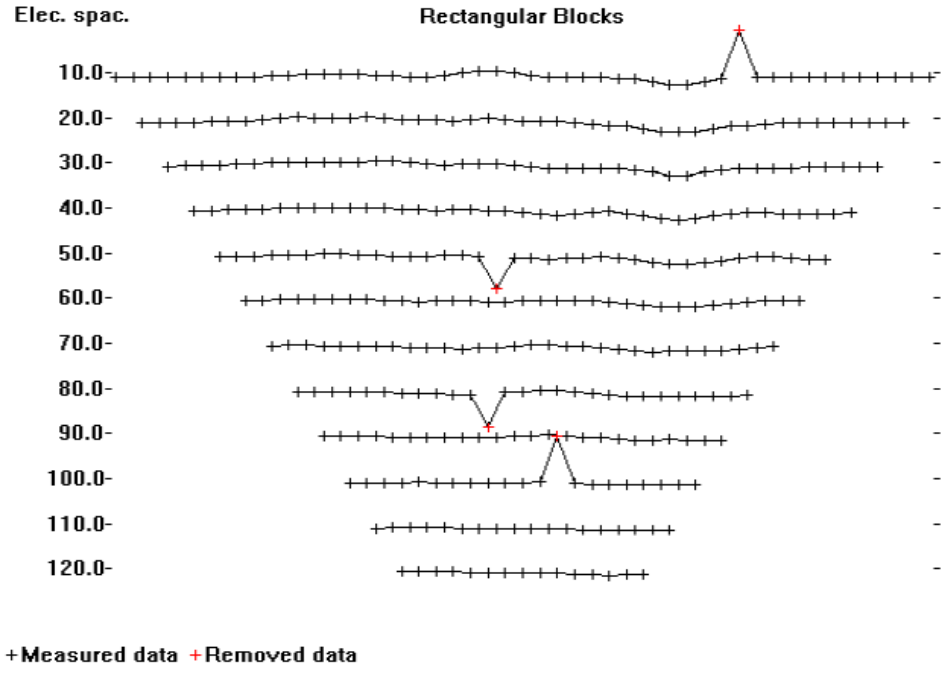

Figure 6.8. Example of a data set with a few bad data points (Loke, 2004)

The software creates a resistivity model/resistivity profile that has the same resistivity distribution as the actual resistivity distribution below the corresponding traverse. To increase the quality of the calculated model, the Root Mean Square (RMS)

method is used, (Loke, 2004). In this method, the smaller the RMS value, the better the calculated model correlates with real resistivity distribution. In this project, an RMS value of 50% was used.

To create a resistivity model, the RES2DINV subdivides the subsurface into a finite number of rectangular pixels. Each pixel is assigned a resistivity value which represents the resistivity of different materials encompassed within that discrete pixel; therefore some lateral and vertical smoothing takes place (Anderson, 2006).

The size of the pixels is affected by the spacing between the adjacent electrodes. Horizontal dimension of a pixel is equal to lateral distance between adjacent electrodes, and at shallow depth, the vertical dimension is approximately equal to 20% of the spacing between two adjacent electrodes. With increasing depth of investigation, the vertical dimension of pixels gradually increases up to 100% of the distance between adjacent electrodes (Anderson et al., 2006). The resolution of the output model is a function of the pixel size (Figure 6.9). Thus, with increasing depth of investigation, resolution decreases.

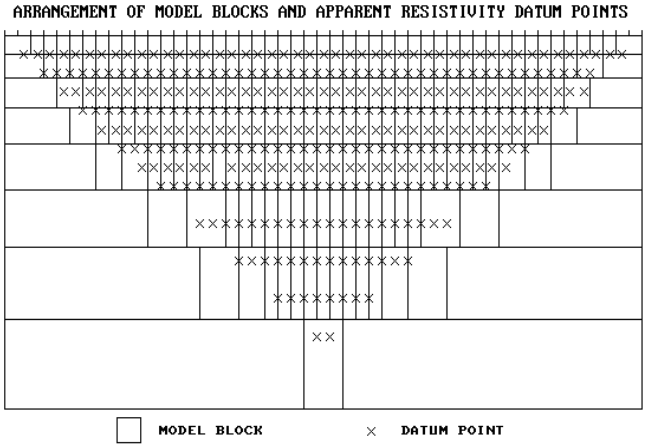

Figure 6.9. Arrangement of the blocks used in a model together with the data points

When a Dipole-dipole array is used, the maximum depth of investigation is approximately 20%-25% of the array length but this is affected by subsurface condition such as the top layer of the ground being very dry. For this project, the depth of investigation was about 36 ft (11m).

The ERT resistivity profiles generated (Figure 6.10 - Figure 6.14) are later interpreted by picking the inverse model resistivity sections.

Caption A (Figure 6.10) is the measured apparent resistivity pseudosection which represents the data set acquired in the field, caption B is the calculated apparent resistivity pseudosection which represents a synthetic model that is used to estimate the size of the pixels at different layers and C represents the Inverse model resistivity section which represents the true geologic model of the subsurface. The unit electrode spacing was 2.5 feet (0.76m).

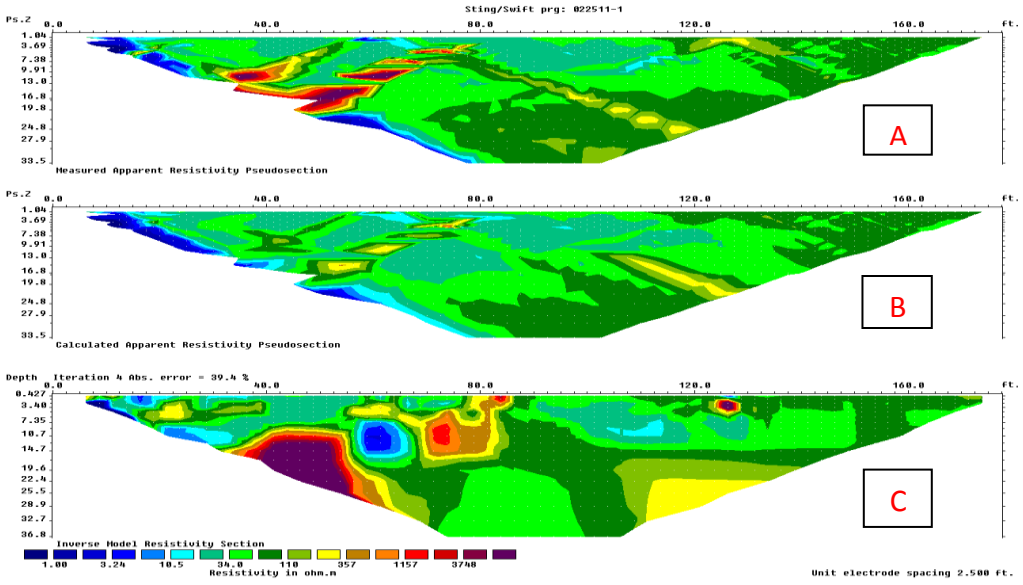

Figure 6.10. Unedited/raw profile 1

Caption A (Figure 6.11) is the measured apparent resistivity pseudosection which represents the data set acquired in the field, caption B is the calculated apparent resistivity pseudosection which represents a synthetic model that is used to estimate the size of the pixels at different layers and C represents the Inverse model resistivity section which represents the true geologic model of the subsurface. The unit electrode spacing was 2.5 feet (0.76m).

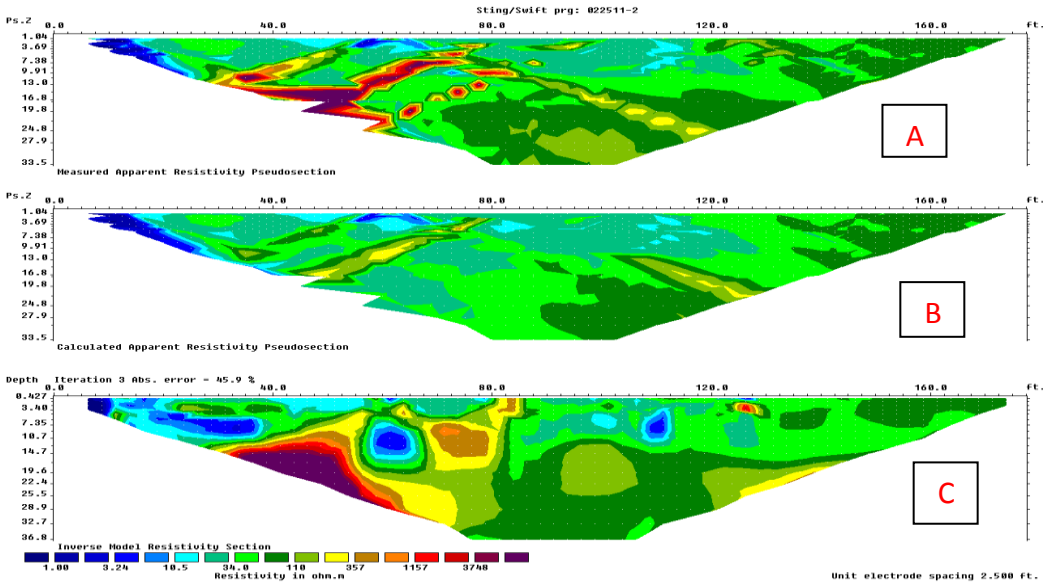

Figure 6.11. Unedited/raw profile 2

Caption A (Figure 6.12) is the measured apparent resistivity pseudosection which represents the data set acquired in the field, caption B is the calculated apparent resistivity pseudosection which represents a synthetic model that is used to estimate the size of the pixels at different layers and C represents the Inverse model resistivity section

which represents the true geologic model of the subsurface. The unit electrode spacing was 2.5 feet (0.76m).

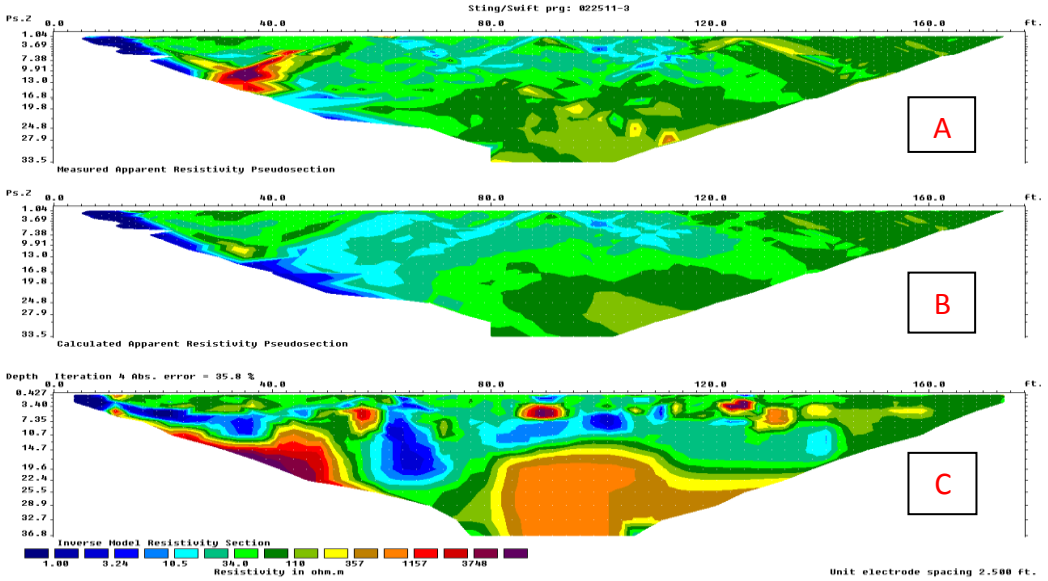

Figure 6.12. Unedited/raw profile 3

Caption A (Figure 6.13) is the measured apparent resistivity pseudosection which represents the data set acquired in the field, caption B is the calculated apparent resistivity pseudosection which represents a synthetic model that is used to estimate the size of the pixels at different layers and C represents the Inverse model resistivity section which represents the true geologic model of the subsurface. The unit electrode spacing was 2.5 feet (0.76m).

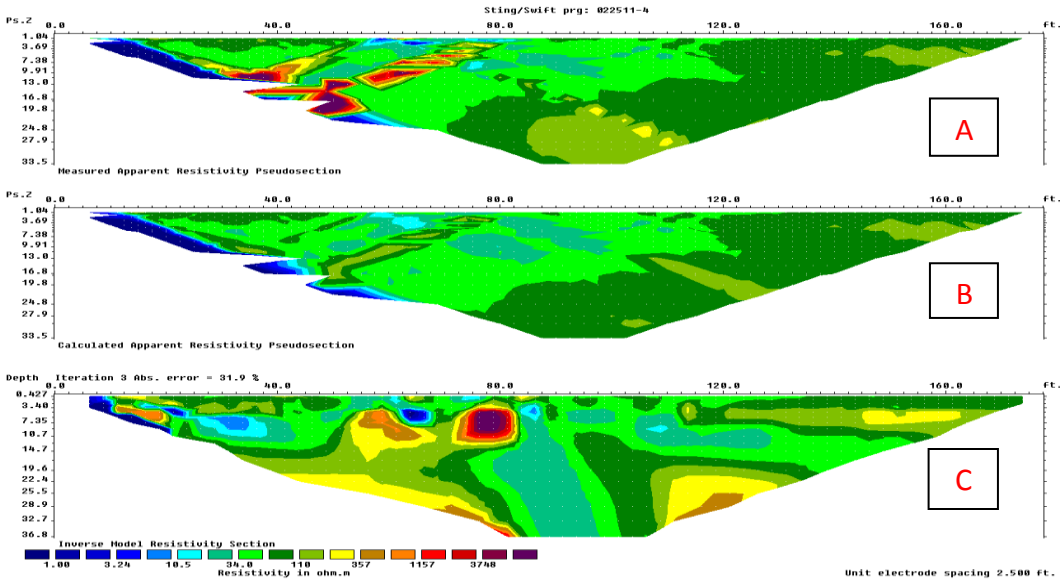

Figure 6.13. Unedited/raw profile 4

Caption A (Figure 6.14) is the measured apparent resistivity pseudosection which represents the data set acquired in the field, caption B is the calculated apparent resistivity pseudosection which represents a synthetic model that is used to estimate the size of the pixels at different layers and C represents the Inverse model resistivity section which represents the true geologic model of the subsurface. The unit electrode spacing was 2.5 feet (0.76m).

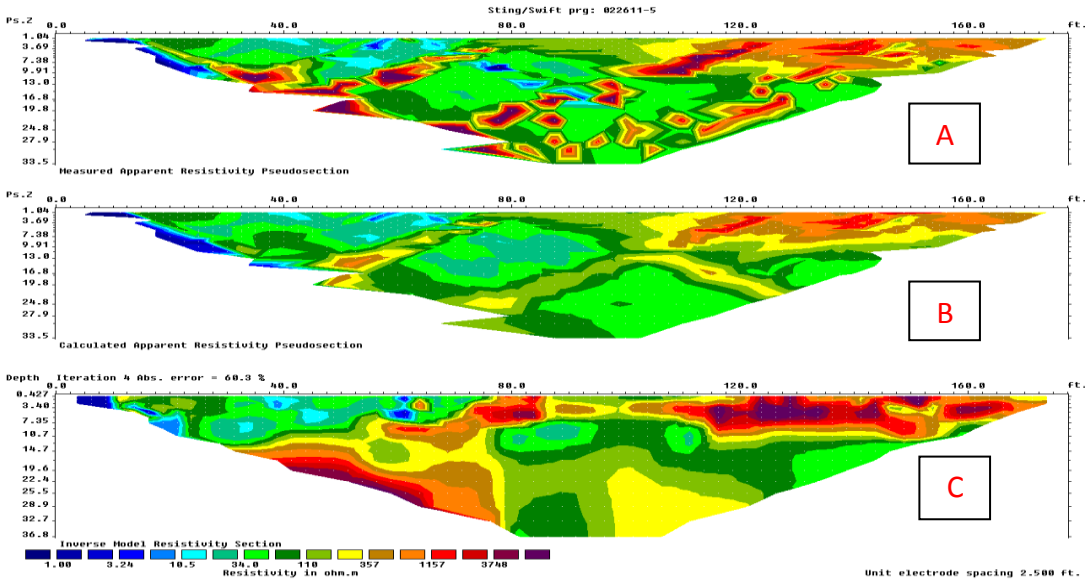

Figure 6.14. Unedited/raw profile 5

6.3. RESOLUTION LIMITATION OF ERT METHOD

Resolution is a function of electrode spacing and resistivity contrast between lithologically different earth materials. The resolution of electrical resistivity tomography (ERT) profile defines the accuracy of interpretation of subsurface conditions. The size of a pixel is a main estimate of ERT imaging resolution. In this thesis, at shallow depth, the width of the pixel is about 2.5ft (0.76m) and the vertical dimension of the pixel is around 0.5ft (0.15m). This means that at this shallow depth, all objects that are less than the size of the pixel will be easily detected. With increasing depth, the vertical dimension of the pixels becomes greater and that reduces ERT resolution. To estimate the size of all detectable objects at a certain depth, it is recommended to compile a synthetic resistivity model. The model can be used to visually estimate the size of the pixels at different depth

layers. During ERT survey, when current is induced to flow through deeper layers, the distance between current and potential electrodes is gradually increased. This affects the sensitivity of the ERT method. Gradually increasing the distance between electrodes lowers the intensity of current flow, and accordingly the sensitivity of ERT survey. Thus, interpretation of smaller scale objects at greater depths becomes increasingly difficult and sometimes small objects can be missed or misinterpreted.

Resistivity contrast is another parameter that defines the resolution of ERT profile. When lithologically different materials exhibit similar conductivity parameters, sometimes it is difficult to differentiate them simply on the basis of their resistivity parameters. For example, both intact bedrock and air-filled voids typically are characterized by high resistivity values. When an air-filled void is embedded in intact limestone, it typically cannot be easily detected on resistivity profile because of low resistivity contrast. In the project site, there are some areas where resistivity measurements were not acquired due to lack of resistivity contrast between the soils and fractured bedrock. Resistivity contrast plays a major role in ERT method, but in a situation where there is no signal due to close resistivity properties between earth materials; borehole information can be used to complement resistivity data.

7. DATA INTERPRETATION

Because of variability in resistivities of earth materials, interpretation of electrical resistivity tomography (ERT) data must be handled with caution. Factors such as temperature, porosity, conductivity, salinity, clay content, saturation and lithology generally affect the resistivity of earth materials. There are also overlaps of the resistivity values of earth materials which in most cases are given as ranges of values rather than absolute values. For example sandstone, limestone, dolomite, sand, and clay have resistivity values that can range from 1 ohm-m to 10^8 ohm-m. For more effective data interpretation, resistivity control for the lithologic materials in the study area would help to reduce any ambiguity.

The objective of this survey was to map the lateral and vertical extent of water-filled vugs near the unnamed bridge foundation at the project site, and possibly locate the top of bedrock in that vicinity. With this, it would be possible to design an appropriate engineering solution such to strengthen the load-bearing capacity of the bridge foundation.

The ERT resistivity profile and model were used for interpretation of subsurface conditions within the study site. This ERT survey was complemented by geotechnical ground sampling obtained from borings. Nine boreholes, designated T-11-03 through T-11-11 were drilled more-or-less along the resistivity traverses for site characterization. The soil encountered in the borings consisted of lean clay and silty alluvium with varying amounts of sand and gravel. The rock encountered on site was typically dolomite of varying degrees of vuggyness and weathering. These results are summarized in Table 7.1.

Table 7.1. Summary of results of boring logs at the project site

Borings								
T-11-03 Depth (ft)	T-11-04 Depth (ft)	T-11-05 Depth (ft)	T-11-06 Depth (ft)	T-11-07 Depth (ft)	T-11-08 Depth (ft)	T-11-09 Depth (ft)	T-11-10 Depth (ft)	T-11-11 Depth (ft)
0-20.5 Soil	0-20.6 Soil	0-18.5 Soil	0-18.5 Soil	0-19.2 Soil	0-22.3 Soil	0-20.5 Soil	0-23.0 Soil	0-20.8 Soil
20.5-21.3 Weathered rock	20.6-21.2 Weathered rock	18.5-28. Vuggy rock	18.5-19.0 Weathered rock	19.2-28.4 Vuggy rock	22.3-22.9 Weathered rock	20.5-22.0 Weathered rock	23.0-25.2 Weathered rock	20.8-31.6 Vuggy rock
21.3-33.0 Hard rock	21.2-27.7 Void		19.0-20.7 Vuggy rock		22.9-27.4 Void	22.0-27.4 Void	25.2-34.2 Vuggy rock	
	28.0-28.5 Rock		20.7-20.9 void		27.4-34.0 Vuggy rock	27.4-34.2 Vuggy rock		
			20.9-23.4 Vuggy rock					
			23.4-27.0 Void					
			27.0-34.2 Vuggy rock					

7.1. GENERAL GUIDE TO ERT DATA INTERPRETATION

Factors such as porosity, conductivity, saturation, salinity, clay content, lithology, and temperature can affect the ability of different materials to conduct electrical current. Accordingly, materials of the same mineral content may exhibit different resistivity values (Table 5.1). For instance, dry soil usually has much higher resistivity than saturated soil. The same situation appears with weathered and unweathered rock. Weathered rock is usually more porous and fractured, and it becomes more saturated with groundwater; as a result, weathered rock has lower resistivity than intact rock.

According to previous studies (Anderson et al., 2006) conducted in southwestern Missouri, typical resistivity values for the subsurface materials are characterized as follows:

- Moist clays in southwestern Missouri are normally characterized by low resistivity values (usually less than 100 ohm-m) and may vary due to different degrees of saturation, porosity, and layer thicknesses.
- Moist soils and intensively fractured rocks intermixed with clay typically have resistivity values between 100 and 400 ohm-m. Such variation is explained by different porosity, saturation, clay content, and layer thicknesses.
- Relatively intact limestone with minimal clay content is characterized by higher resistivity values, typically more than 400 ohm-m. Resistivity values of intact limestone may vary due to varying layer thickness, moisture content, porosity, saturation, and impurities.
- Air-filled cavities usually show very high resistivity values, usually more than 1000 ohm-m, but again, are variable depending on the conductivity of the surrounding strata and depth/size/shape of void. Zones where relatively intact bedrock is surrounded by moist loose materials (such as clay), or zones where air-filled voids are embedded in relatively intact limestone, are zones of electrical resistivity contrast. These zones can be successfully detected by electrical resistivity tools.

The following explanations are necessary in ERT data interpretation.

The apparent resistivity is a term used for the field measurement, since without interpretation; the resistivity measurement does not refer to any particular geologic layer. The resistivity pseudosection produced consists of the measured apparent resistivity pseudosection, the calculated apparent resistivity pseudosection and the inverse model resistivity section. In this case, they are referred to as raw or unedited

profiles. In order to interpret a profile, say profile 1; the profile has to be edited. In that case, the inverse resistivity model is picked and interpreted because it represents the actual geologic model of the subsurface; which gives information on the vertical distribution of layer thicknesses, depths and resistivities (Figure 7.1-Figure 7.5).

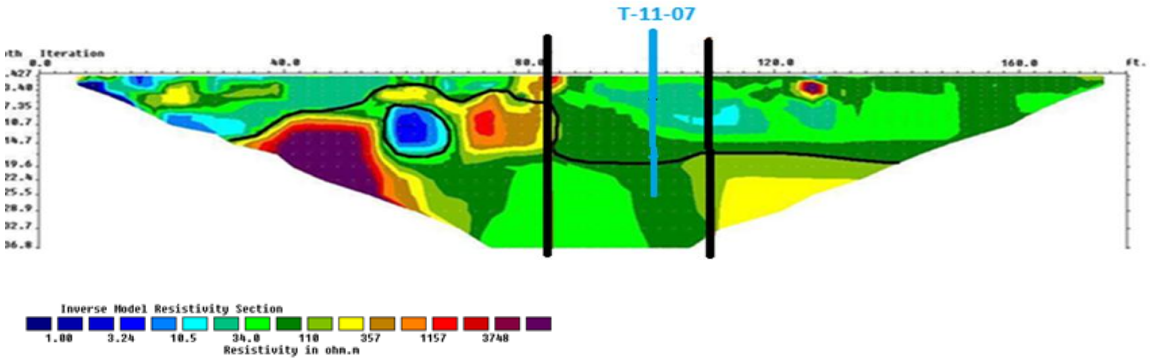

Figure 7.1. Interpreted profile 1

The black line indicates the interpreted top of bedrock; the resistivity value is less than 400 ohm-m, this is based on studies conducted in southwestern Missouri (Anderson et al., 2006) which showed that intensively fractured rocks intermixed with clay are typically of resistivity values between 100 and 400 ohm-m. The rock is also highly saturated. This is consistent with borehole control, where borehole T-11-07 was drilled along traverse 1. The blue color with resistivity value less than 10 ohm-m appears to represent a sediment/clay-filled vug , this is based on studies conducted in southwestern

Missouri where moist clays are normally characterized by low resistivity values usually less than 100 ohm-m. The result shows that bedrock dips steeply from east to west.

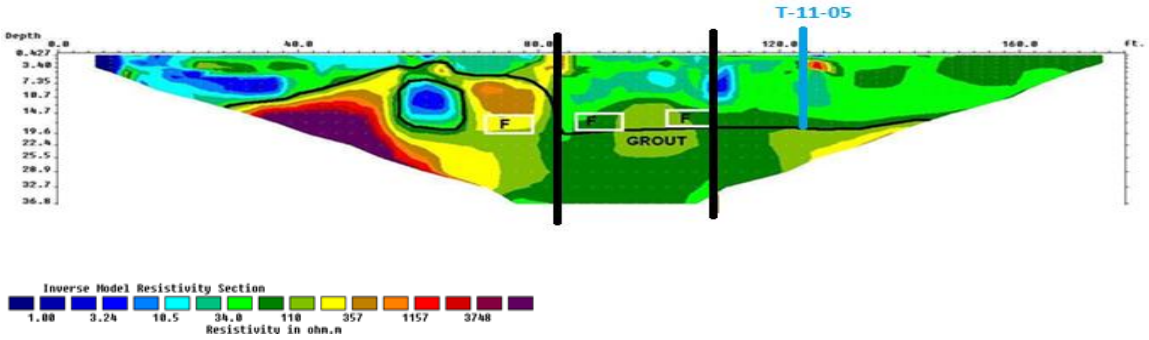

Figure 7.2. Interpreted profile 2

The superposed black line indicates the interpreted top of bedrock, the resistivity value is less than 400 ohm-m, this is based on studies conducted in southwestern Missouri (Anderson et al., 2006) which showed that intensively fractured rocks intermixed with clay typically have resistivity values between 100 and 400 ohm-m. Resistivity value of about 110 ohm-m was recorded. The rock is also highly saturated; this is consistent with borehole control T-11-05. The blue spots appear to be sediment/clay-filled vugs with resistivity values less than10 ohm-m, this is based on studies conducted in southwestern Missouri (Anderson et al., 2006) where moist clays are normally characterized by low resistivity values usually less than 100 ohm-m. Bedrock dips from east to west.

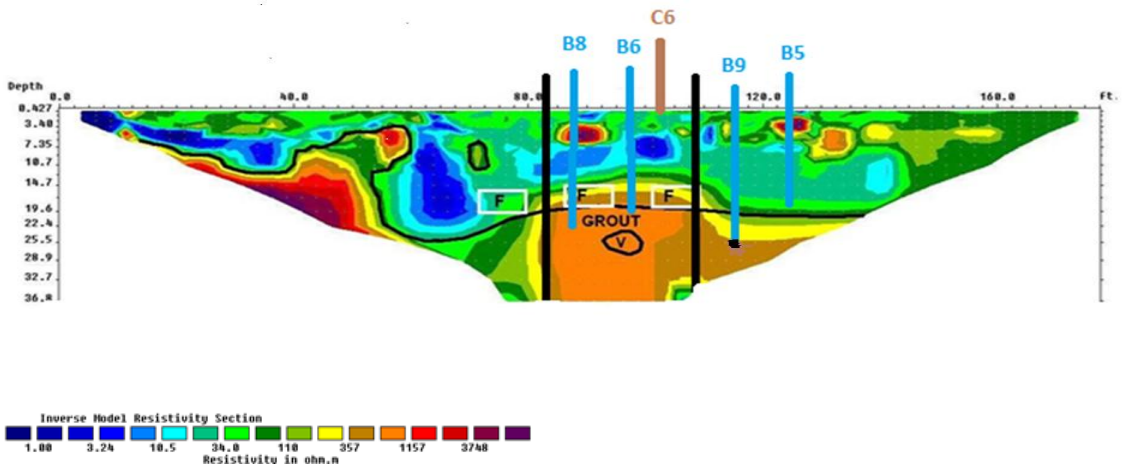

Figure7.3. Interpreted profile 3

The bridge pier, C6 is the primary exploration target, as such; four boreholes (B5, B6, B8, and B9) which are designated as T-11-05, T-11-06, T-11-08 and T-11-09 in boring table (Table 7.1) were drilled along traverse 3. The superposed black line indicates the interpreted top of bedrock, a resistivity value of around 110 ohm-m was recorded, indicating that the top of the bedrock is highly fractured; this is based on studies conducted in southwestern Missouri (Anderson et al., 2006) which showed that intensively fractured rocks intermixed with clay typically have resistivity values between 100 and 400 ohm-m. The bedrock here appears to be competent bedrock, with resistivity value more than 1000 ohm-m. Void was encountered on this profile, and according to studies in southwestern Missouri (Anderson et al., 2006), air-filled cavities usually show very high resistivity values, usually more than 1000 ohm-m, but again, are variable, depending on the conductivity of the surrounding strata and depth/size/shape of void.

The high resistivity value could also be as a result of the grout placed below the footing years ago. Voids were encountered in boreholes B6, B8 and B9; this is consistent with borehole control. The blue spots appear to be sediment/clay-filled vugs with resistivity values less than10 ohm-m. This is based on studies conducted in southwestern Missouri where moist clays are normally characterized by low resistivity values usually less than 100 ohm-m (Anderson et al., 2006).

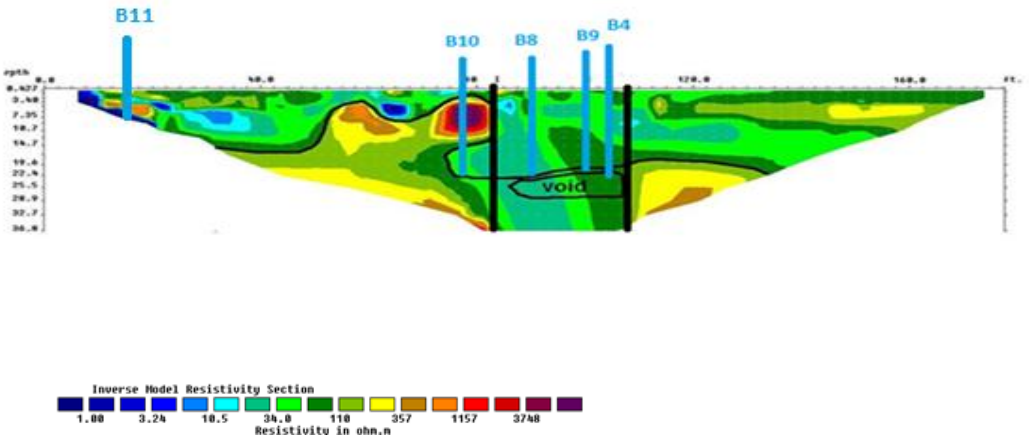

Figure 7.4. Interpreted profile 4

The superposed black line indicates the interpreted top of bedrock .Void was encountered on this traverse; this is consistent with borehole control where B4, B8 and B9 designated as T-11-04, T-11-08 and T-11-09 in the boring log encountered voids (Table7.1). Sediment/clay-filled vugs were few and small in sizes, with resistivity values

less than10 ohm-m. A high resistivity value above 3700 ohm-m observed, appears to be gravel.

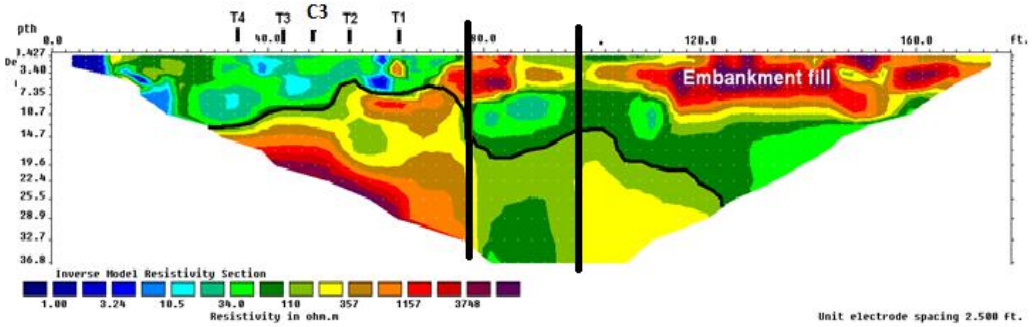

Figure 7.5. Interpreted profile 5

In this profile, T1, T2, T3 and T4 are positions of ERT profiles 1, 2, 3 and 4 with respect to profile 5, and C3 is the position of bridge pier 3. This profile is orthogonal in direction with the rest of the traverses; no borehole was drilled along this traverse as at the time of this project. The black line indicates the top of bedrock with resistivity value of about 110 0hm-m, this is based on studies conducted in southwestern Missouri (Anderson et al., 2006) which showed that intensively fractured rocks intermixed with clay typically have resistivity values between 100 and 400 ohm-m. Sediment/clay-filled vugs are few and small in sizes with resistivity values less than10 ohm-m. High resistivity value above 3700 ohm-m observed, appears to be saturated gravel used as embankment fill.

Geophysical data, along with boring information was used to interpret the subsurface conditions; consequently, the following conclusions were made:

- Bedrock beneath the bridge pier is generally characterized by resistivity values of less than 400 ohm-m, except on ERT profile 3 in immediate proximity to the columns, where resistivity value up to 1000 ohm-m was observed. This relatively low resistivity of bedrock is an indication that this rock is extensively fractured and saturated.
- Top of bedrock in proximity to the pier is interpreted as being at a shallow depth to the east of the structure (based on ERT profile1) and at depths on the order of 20 feet (6m) immediately to the west of the structure . This indicates that bedrock dips steeply from east to west beneath the pier.
- The top of bedrock cannot be mapped with confidence on all the ERT profiles due to the fact that interpreted fractured rock, in most places, is characterized by resistivity values that are the same as the overlying soil. In places where they are mapped, the top of bedrock is at a depth of around 20 feet (6m); this is consistent with borehole control (Table 7.1).
- At the eastern side of the pier, bedrock beneath the pier is generally characterized by resistivity values of between 400 and 4000 ohm-m, and is interpreted as competent rock except where shallow gravels appear to be present.

7.2. ENGINEERING SOLUTION APPLIED

Compaction grouting was the engineering solution employed to seal the voids, and was based on the result of ERT and boreholes drilled at the project site (Table 7.2).

Table 7.2. Summary of sizes of voids and volume of grout used to seal the voids

Borehole	Total depth (ft.)	Range of voids (ft.)	Vertical extent (ft.)	Volume of grout placed (cu.ft.)
T-11-04	28.5	21.2-27.7	6.5	378
T-11-06	34.2	20.7-27.0	3.8	410.4
T-11-08	34.0	22.9-27.4	4.5	506.2
T-11-09	34.2	22.0-27.4	5.4	492.7
BW-1	34.2	Not logged	Not logged	26.9
BW-2	29.2	Not logged	Not logged	13.5
BW-3	N/A	Not logged	Not logged	Drilling aborted
BW-3a	25.0	Not logged	Not logged	378.0
SW-1	27.5	Not logged	Not logged	6.7
Total Volume of grout used: 2212.4 cubic feet = 81.94 cubic yards.				

Based on the result of the borings and ERT, voids were detected in nine boreholes drilled along resistivity traverses close to the bridge pier in question (C6) as shown in Table 7.2. The voids were grouted using compaction grouting technique. Compaction grouting, also known as low mobility grouting is a grouting technique that displaces and densifies loose granular soils, reinforces fine grained soils and stabilizes subsurface voids or sinkholes. This is usually done by injecting low-slump, low-mobility aggregate grout using an injection pipe. From the result of the grouting program, a total volume of about 2212.4 cubic feet (81.94 cubic yards) of grout was used to seal the voids and stabilize the ground around the structure.

The result of the interpretation of the five ERT profiles acquired showed a linear topographic feature (Figure 7.6) that is believed to reflect groundwater flow direction. Groundwater is continually moving, often very slowly. The movement is controlled by gravity, topography and geology. Gravity is the major driving force and thus groundwater is always moving from areas of higher elevation to lower elevation. The project site has an undulating topography which controls groundwater movement. Another important factor that controls groundwater movement in this area is the nature of rock formations that are found in the area. Rock formations in the area are predominantly dolomite (Gasconade dolomite) which dissolves in slightly acidic waters; the dissolved materials, along with the remaining insoluble parts of the rock are transported from the site through solution enlarged openings in the bedrock. Also, the top of bedrock in the project site is highly fractured, so fracture is also a factor in groundwater flow direction in the site.

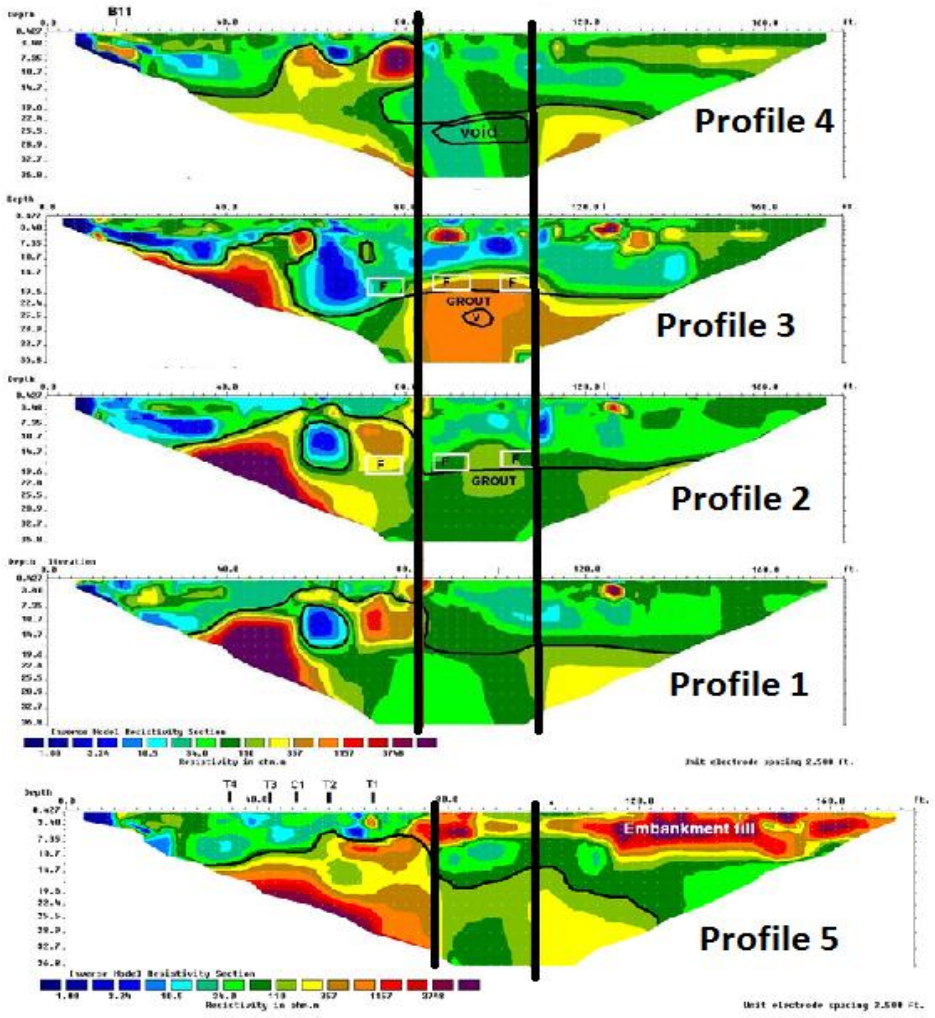

Figure 7.6. Lineament showing horizontal bedding plane

The interpretation is consistent with borehole data which shows that voids occur approximately at the same depth of around 22 feet (6.7m). This lineament as (Figure 7.6) is an indication that solution cavities encountered beneath the bridge developed most probably along horizontal bedding planes rather than vertical bedrock joints.

8. CONCLUSION

A structural support was needed to strengthen the load-bearing capacity of a bridge foundation in Laclede County in South-Central Missouri due to increasing volume of traffic and age of the bridge (constructed in 1955). During the construction of a drilled shaft for the substructure a few feet north of the north footing of the pier, voids were noted beneath a roughly 2 - foot (0.6m) - thick cap of dolomite rock near the bridge. Water - filled voids were also observed very close to the bridge pier. Because of these, there were concerns about the integrity of the rock beneath the existing bridge foundation, and had to be mapped to determine the extent of the voids.

In order to map the lateral and vertical extent of the voids, as well as locate the top of bedrock near the bridge foundation, electrical resistivity tomography (ERT) was deemed the appropriate geophysical tool to be used for site characterization, complemented by borehole information (borehole control). The result of this survey was used to determine the proper engineering solution to be employed to achieve this purpose.

According to the results obtained, the following conclusions were made:

- Solution cavities encountered beneath the bridge are limited in size and extent. They developed most probably along horizontal bedding planes rather than vertical bedrock joints, and are likely to be partially clay-filled.
- The ERT survey did not show any room-sized void, showing that the voids are limited in size and extent based on the volume of grout used (2212.4 cubic feet/81.94 cubic yards) to seal the voids.

- The voids present on site appear to be filled with dirty water and as such exhibit resistive properties very close to the surrounding vuggy rock.

Choosing the appropriate geophysical method and constraining it with ground truth from borings will enhance site characterization for geotechnical practice. The choice of method to use depends on a number of factors such as the size and depth of anticipated voids, reason for delineating voids, desired resolution of voids, nature of background materials or bedrock surrounding the voids, type of materials that may fill the voids (such as clay or water), depth to groundwater, size of the investigation area and sources of cultural interference in the investigation area. In some cases, different electrode configurations used in electrical resistivity tomography (ERT) method show similar results especially in a site that is uniform, though each configuration has advantages and disadvantages depending on the physical properties of the host environment and the desired target. Cultural interference in this context refers to power lines and fences which affects resistivity measurements when present at project site. Because power lines and fences are conductive, and conductivity is an inverse of resistivity, these materials lower the resistivity of earth materials in the investigation area, thereby giving inaccurate resistivity measurements.

BIBLIOGRAPHY

Advanced Geosciences, Inc., "Instruction Manual for the SuperSting with Swift Automatic Resistivity and IP System," 2011.http://www.agiusa.com.

Aley, Thomas J., Williams, James H., Massello and James W., "Groundwater Contamination and Sinkhole Collapse Induced by Leaky Impoundments in Soluble Rock Terrain," Missouri Geological Survey and water Resources, Engineering Geology Report; Number 5, 1972.

Edwin S. Robinson, "Current lines Radiating from the Source Electrode and Converging on the Sink Electrode," Field Geophysics, Open University Press and Halsted press Inc., 1989.

Encyclopedia of Caves and Karst Science, "Geophysical Detection of Caves and Karstic Voids," ISBN: 0-203-48385-5, January 2004.

Geotomo Software Malaysia, "Geoelectrical Imaging 2D & 3D, RES2DINV, Ver 3.56," 2011. www.geoelectrical.com.

Haobin Dong, Chuanlei Wang, Huaping Wang, Xinhui Cai and C. Richard Liu, "Two-Dimensional Resistivity Imaging Survey for Detecting Termitaria in a Dam" 2011.http://ieeexplore.ieee.org/stamp/stamp.jsp?tp=&arnumber=1673257&userType=inst.

Hiltunen, D. R., and Roth, M. J. S., "Investigation of Bridge Foundation Sites in Karst Terrains via Multi –Electrode Electrical Resistivity," 2011. http://www.dot.state.fl.us/statematerialsoffice/geotechnical/conference/materials/hiltunen-roth.pdf.

James A. Martin, Robert D. Knight and William C. Hayes "The Stratigraphic Succession in Missouri; Ordovician System," Missouri Geological Survey and Water resources, 1961.

James E. Vandike, "Geologic and Stratigraphic Units in Laclede County," Missouri Geological Survey and Water Resources, 1993.

James W.Duley, John W.Whitfield, Ardel W.Rueff and James E.Vandike, "Geologic and Hydrologic Resources of Laclede County, Missouri, open file Report," 1992.

K. Michael Garman and Scott Purcell, "Three-Dimensional Electrical Resistivity Surveys to Identify Buried Karst Features Affecting Road projects," 2011. http://www.dot.state.fl.us/statematerialsoffice/geotechnical/conference/materials/garman-purcell.pdf.

Karst Map of the US, Published by AGI, http://www.caves.org/pub/journal/pdf/V64/V64n1-Veni.pdf. 2011.

Loke, M. H., "Electrical Imaging Surveys for Environmental and Engineering Studies," 2011. http://www.terraip.co.jp/lokenote.pdf, Pp 445-478.

Neil L. Anderson, Derek B.Apel and Ahmed Ismail "Assessment of Karst Activity At Highway Construction Sites Using the Electrical Resistivity Method," unpublished report for MoDOT, 2006.

P.J. Gibson, P. Lyle, and D.M.George, "Application of Resistivity and Magnetometry Geophysical Techniques for near-surface Investigation in Karstic Terrains in Ireland,"Journal of Cave and Karstic Studies; Volume 39, August 2004; pp 35-38.

Steve Cardimona, "Electrical Resistivity Technique for Subsurface Investigation," 2011. http://citeseerx.ist.psu.edu/viewdoc/download?doi=10.1.1.135.2978&rep=rep.

Taylor and Francis, "Geophysical Detection of Caves and Karstic Voids," Encyclopedia of Caves and Karst Science, 2011.

Umar Hamzah, Rahman Yaacup, Abdul Rahim Samsudin, Mohd Shahid Ayub "Electrical Resistivity Imaging of the Groundwater Aquifer at Banting, Selangor, Malaysia," Journal of Environmental Geology; Volume 49, Number 8/April, 2006; pp1156-1162.

Wallace B. Howe and John Koenig, "The Stratigraphic Succession in Missouri," Volume XL, Second Series, Missouri Geological Survey and Water Resources, 1961.

Wanfang Zhou, Barry F. Beck and Angela L. Adams, "Effective Electrode Array in Mapping Karst Hazards in Electrical Resistivity Tomography," Journal of Environmental Geology; Volume 32, Number 8/ November, 2002; pp 922-928.

W. Zhou, B. F. Beck, and J.B. Stevenson, "Reliability of Dipole-Dipole electrical Resistivity Tomography for Defining Depth to Bedrock in Covered Karst Terrains," Journal of Environmental Geology; Volume 39, Number 7/May, 2000; pp 760-766.

VITA

Jeremiah Chukwunonso Obi was born in Ogidi, Anambra State, Nigeria. He received his Bachelors degree (BSc.hons.) in Geological Sciences in 1997 from Nnamdi Azikiwe University Awka, Nigeria. He moved to the United States in 2008, worked for some time and got admission into Missouri University of Science and Technology where he received his Masters degree (M.S.) in Geological Engineering in May 2012.